Mean-field underdamped Langevin dynamics and its spacetime discretization

Qiang Fu[*]　　　　　Ashia Wilson[†]

fuqiang7@mail2.sysu.edu.cn　　ashia07@mit.edu

[*]School of Mathematics, Sun Yat-sen University
[†]Department of Electrical Engineering and Computer Science, MIT

Abstract

We propose a new method called the N-particle underdamped Langevin algorithm for optimizing a special class of non-linear functionals defined over the space of probability measures. Examples of problems with this formulation include training mean-field neural networks, maximum mean discrepancy minimization and kernel Stein discrepancy minimization. Our algorithm is based on a novel spacetime discretization of the mean-field underdamped Langevin dynamics, for which we provide a new, fast mixing guarantee. In addition, we demonstrate that our algorithm converges globally in total variation distance, bridging the theoretical gap between the dynamics and its practical implementation.

1 Introduction

The mean-field Langevin dynamics (MLD) has recently received renewed interest due to its connection to gradient-based techniques used in supervised learning problems such as training neural networks in a limiting regime (Mei et al., 2018). Theoretical characterizations of the convergence properties of MLD has been the particular focus of several recent works (Hu et al., 2019; Chizat, 2022; Nitanda et al., 2022; Chen et al., 2022; Claisse et al., 2023). More generally, MLD can be used to solve problems that can be posed as an entropy regularized mean-field optimization (EMO) problem. Other examples of such problems include density estimation via maximum mean discrepancy (MMD) minimization (Gretton et al., 2006; Arbel et al., 2019; Chizat, 2022; Suzuki et al., 2023) and sampling via kernel Stein discrepancy (KSD) minimization (Liu et al., 2016; Chwialkowski et al., 2016; Suzuki et al., 2023). A more detailed synthesis of recent theoretical developments for MLD can be summarized as follows. Hu et al. (2019) show that MLD finds EMO solutions asymptotically when problems can be expressed as optimizing a convex functional. If in addition, the EMO satisfies a uniform logarithmic Sobolev inequality, several studies have established that this convergence occurs exponentially quickly (Chizat, 2022; Nitanda et al., 2022; Chen et al., 2022).

However, implementing MLD is not a straightforward task; to arrive at a practical algorithm requires both spatial and temporal discretizations of the dynamics. Nitanda et al. (2022) study a time-discretization of MLD by extending an interpolation argument introduced by Vempala and Wibisono (2019) to a non-linear Fokker-Planck equation. They establish a non-asymptotic rate of convergence for the discrete-time process. Chen et al. (2022) study a space-discretization consisting of a finite-particle approximation to the density of MLD (referred to as a finite-particle system) and show the finite-particle system finds the solution to the EMO problem exponentially fast, with a bias related to the number of particles. More practically, Suzuki et al. (2023) analyze a spacetime discretization of the MLD and establish the non-asymptotic convergence of the resulting algorithm to a biased limit related to both the number of particles used and stepsize. Their analysis applies to several important learning problems and improves the results of the standard gradient Langevin dynamics. A natural candidate method for finding solutions to EMO problems faster

is the mean-field *underdamped* Langevin dynamics (MULD). MULD resemble several techniques for adding momentum to gradient descent in optimization, many of which are known to result in provably faster convergence in a variety of settings (Nesterov, 1983; Wilson et al., 2016; Laborde and Oberman, 2020; Hinder et al., 2020; Fu et al., 2023). Moreover, training neural networks using momentum-based gradient descent is considered effective in several applications (Sutskever et al., 2013; Kingma and Ba, 2014; Ruder, 2016). Kazeykina et al. (2020) and Chen et al. (2023) confirm that a naive spacetime discretization of MULD has impressive empirical performance when compared to a naive discretization of the MLD on applications such as training mean-field neural networks. Chen et al. (2023) introduce a space-discretization of MULD consisting of a finite particle approximation to the density and show it finds the EMO solution exponentially fast, albeit with several additional assumptions that are easy to verify for the problem of training mean-field neural networks. In addition, Chen et al. (2023) implement an Euler-Maruyama discretization of the finite-particle system and show that it performs empirically faster when compared with the spacetime discretization of the mean-field Langevin dynamics in training a toy neural network model. However, spacetime discretizations of MULD are not yet theoretically well understood. Furthermore, the rate obtained by Chen et al. (2023) for the dynamics does not resemble an "accelerated rate" when compared with recent results for MLD.

A summary of our work

A remaining question is whether we can theoretically characterize the behavior of an implementable algorithm based on discretizing the mean-field underdamped dynamics. If there is a limiting bias, how does it scale with the number of particles and other problem parameters? Ideally, this characterization would give a sharper rate of convergence than Suzuki et al. (2023)'s spacetime discretization of the mean-field Langevin dynamics, suggesting there might be an advantage to adding momentum in the mean-field setting (at least in the worst case). In this paper, we introduce a fast implementable algorithm for solving EMO problems based on the mean-field underdamped Langevin dynamics. We prove that our proposed algorithm converges to a small limiting bias under a set of assumptions that subsumes many problems of interest. In particular, our contributions are summarized as follows.

1. We sharpen the convergence bound for MULD and its space-discretization established by Chen et al. (2023) under the same set of assumptions utilized by Chen et al. (2023) (Theorems 3.1 and 3.2 and Table 1).

2. We show the global convergence of our proposed algorithm in total variation (TV) distance (Theorem 3.4). Importantly, our results improve on Suzuki et al. (2023)'s analysis of the space-time discretization of the MLD. While we require additional assumptions 2.5-2.7, our results hold in several real-world applications including training neural networks, density estimation via MMD minimization and sampling via KSD minimization.

Organization The remainder of this work is organized as follows. Section 2 presents the formal definitions and assumptions as well as important related work. Section 3 proposes our main methods and theoretical results. Section 4 discusses the application of our methods to some classical problems. Section 5 describes our numerical experiments verifying the effectiveness of our proposed methods.

2 Preliminaries

We begin by introducing some general notation that will be used throughout this work.

2.1 Notation

The Euclidean and operator norms are denoted by $\|\cdot\|$ and $\|\cdot\|_{\mathsf{op}}$. The space of probability measures on $\mathbb{R}^d$ with finite second moment is denoted by $\mathcal{P}_2(\mathbb{R}^d)$. Throughout, let ρ and μ denote general distributions in $\mathcal{P}_2(\mathbb{R}^d)$ and $\mathcal{P}_2(\mathbb{R}^{2d})$ respectively. The TV distance between ρ and $\pi \in \mathcal{P}_2(\mathbb{R}^d)$ is denoted by $\|\rho - \pi\|_{\mathsf{TV}} := \sup |\rho(A) - \pi(A)|$ where the sup is over all Borel measurable sets $A \subset \mathbb{R}^d$. The p-Wasserstein distance and Kullback-Leibler divergence between ρ and π is denoted by $W_p(\rho, \pi) := \inf_\Pi \mathbb{E}_\Pi[\|x - y\|^p]^{1/p}$ where the infimum is over joint distributions Π of (x, y) with the marginals $x \sim \rho, y \sim \pi$ and $\mathsf{KL}(\rho\|\pi) := \int \rho \log \frac{\rho}{\pi}$. The relative Fisher information is denoted by $\mathsf{FI}(\rho\|\pi) := \mathbb{E}_\rho \|\nabla \log \frac{\rho}{\pi}\|^2$, and more generally we use the notation $\mathsf{FI}_S(\rho\|\pi) := \mathbb{E}_\rho \|S^{1/2}\nabla \log \frac{\rho}{\pi}\|^2$ for a positive definite symmetric matrix S. $\mathrm{Ent}(\rho) := \int \rho \log \rho$ denotes the negative entropy of ρ. The functional and intrinsic derivatives of F are denoted by $\frac{\delta F}{\delta \rho} : \mathcal{P}_2(\mathbb{R}^d) \times \mathbb{R}^d \to \mathbb{R}$ and $D_\rho F := \nabla \frac{\delta F}{\delta \rho} : \mathcal{P}_2(\mathbb{R}^d) \times \mathbb{R}^d \to \mathbb{R}^d$, respectively. A d-dimensional Brownian motion is denoted by B_t. We use notation $a \lesssim b$, $a_n = \Theta(b_n)$ and $a_n = \widetilde{\Theta}(b_n)$ to denote that there exist $c, C > 0$ such that $a \leq Cb$, $cb_n \leq a_n \leq Cb_n$ for $n \geq N'$ and $a_n = \Theta(b_n)$ up to logarithmic factors, respectively.

2.2 Background

We consider the following problem described by minimizing the entropy regularized mean-field objective (EMO),

$$\min_{\rho \in \mathcal{P}_2(\mathbb{R}^d)} F(\rho) + \lambda \mathrm{Ent}(\rho), \tag{1}$$

where $F : \mathcal{P}_2(\mathbb{R}^d) \to \mathbb{R}$ is a potentially non-linear functional and $\lambda > 0$ is a regularization constant. Without loss of generality, we will take $\lambda = 1$ throughout. Hu et al. (2019) study the gradient flow dynamics of the EMO in 2-Wasserstein metric called the *mean-field Langevin dynamics* (MLD):

$$\mathrm{d}x_t = -D_\rho F(\rho_t, x_t)\mathrm{d}t + \sqrt{2}\mathrm{dB}_t, \tag{MLD}$$

where $\rho_t := \mathrm{Law}(x_t) \in \mathcal{P}_2(\mathbb{R}^d)$. Under mild conditions, the MLD finds the solution to the EMO, given by $\rho_*(x) \propto \exp\left(-\frac{\delta F}{\delta \rho}(\rho_*, x)\right)$ (Hu et al., 2019).

This paper introduces a new sharp mixing-time bound for the *mean-field underdamped Langevin dynamics* (MULD):

$$\begin{aligned} \mathrm{d}x_t &= v_t\mathrm{d}t, \\ \mathrm{d}v_t &= -\gamma v_t\mathrm{d}t - D_\rho F(\mu_t^X, x_t)\mathrm{d}t + \sqrt{2\gamma}\mathrm{dB}_t. \end{aligned} \tag{MULD}$$

Here, $\mu_t := \mathrm{Law}(x_t, v_t) \in \mathcal{P}_2(\mathbb{R}^{2d})$, $\gamma > 0$ is the damping coefficient, and $\mu_t^X := \mathrm{Law}(x_t) = \int \mu_t(x, v)\mathrm{d}v$ is the X-marginal of μ_t. The limiting distribution of MULD is the solution to the augmented EMO problem,

$$\min_{\mu \in \mathcal{P}_2(\mathbb{R}^{2d})} F(\mu^X) + \mathrm{Ent}(\mu) + \int \frac{1}{2}\|v\|^2 \mu(\mathrm{d}x\mathrm{d}v), \tag{2}$$

where a momentum term is added to the EMO. The minimizer of the augmented EMO is given by $\mu_*(x, v) \propto \exp\left(-\frac{\delta F}{\delta \rho}(\mu_*^X, x) - \frac{1}{2}\|v\|^2\right)$. We provide details of the derivation of the limiting distributions of MLD and MULD in Appendices A.1 and A.3 respectively. To obtain the solution of the EMO problem, the minimizer $\mu_*(x, v)$ can be X-marginalized. This work also sharpens the analysis of the space-discretization of MULD introduced by Chen et al. (2023), which we refer to

as the *N-particle underdamped Langevin dynamics* (N-ULD) for $i = 1, ..., N$:

$$\mathrm{d}x_t^i = v_t^i \mathrm{d}t, \tag{N-ULD}$$
$$\mathrm{d}v_t^i = -\gamma v_t^i \mathrm{d}t - D_\rho F(\mu_{\mathbf{x}_t}, x_t^i)\mathrm{d}t + \sqrt{2\gamma}\mathrm{dB}_t^i,$$

where $\mu_{\mathbf{x}_t} := \frac{1}{N}\sum_{i=1}^N \delta_{x_t^i}$, $\mu_t^i := \mathrm{Law}(x_t^i, v_t^i)$ and $(\mathrm{B}_t^i)_{i=1}^N$ are d-dimensional Brownian motions.

To motivate our algorithm as a time-discretization of N-ULD, we review discretizations of the *underdamped Langevin dynamics* (ULD), which is a special case of MULD where $F(\mu) = \int V(x)\mu(\mathrm{d}x)$ is a linear functional of μ:

$$\mathrm{d}x_t = v_t \mathrm{d}t \tag{ULD}$$
$$\mathrm{d}v_t = -\gamma v_t \mathrm{d}t - \nabla V(x_t)\mathrm{d}t + \sqrt{2\gamma}\mathrm{dB}_t.$$

The ULD was first studied in Kolmogoroff (1934) and Hörmander (1967). Under functional inequalities such as Poincaré's inequality on the target distribution $\rho_* \propto \exp(-V)$, the convergence guarantee of the ULD was studied by Villani using a hypocoercivity approach Villani (2001, 2009), but without capturing the acceleration phenomenon when compared to the overdamped Langevin dynamics. Cao et al. (2023) are the first to show ULD converges in χ^2-divergence at an accelerated rate when V is convex and the target distribution ρ_* satisfies LSI defined in (5) with $\mathscr{C}_{\mathsf{LSI}} > 0$. They prove that when $\mathscr{C}_{\mathsf{LSI}} \ll 1$, the decaying rate of ULD is $O(\sqrt{\mathscr{C}_{\mathsf{LSI}}})$ whereas the decaying rate of the overdamped Langevin dynamics is $O(\mathscr{C}_{\mathsf{LSI}})$.

A discretization of ULD is referred to as an *underdamped Langevin Monte Carlo* (ULMC) algorithm. There are various discretization schemes proposed for implementing ULD. The *Euler-Maruyama* (EM) discretization of ULD (Kloeden et al., 1995; Platen and Bruti-Liberati, 2010),

$$x_{k+1} = x_k + hv_k, \tag{EM-ULMC}$$
$$v_{k+1} = (1 - \gamma h)v_k - h\nabla V(x_k) + \sqrt{2\gamma h}\xi_k,$$

for stepsize h, $\xi_k \sim \mathcal{N}(0, I_d)$ and $t \in [kh, (k+1)h]$, has been well-studied and it incurs the largest discretization error in several metrics including KL divergence and Wasserstein distance. Recently, however, several works have studied the ULMC obtained from a more precise discretization scheme called the the *exponential integrator* (EI) (Cheng et al., 2018):

$$\mathrm{d}x_t = v_t \mathrm{d}t, \tag{EI-ULMC}$$
$$\mathrm{d}v_t = -\gamma v_t \mathrm{d}t - \nabla V(x_{kh})\mathrm{d}t + \sqrt{2\gamma}\mathrm{dB}_t,$$

for $t \in [kh, (k+1)h]$. Unlike the EM integrator, EI only fixes the drift term in each small interval, creating a group of linear stochastic differential equations (SDE) that can be exactly integrated. Leimkuhler et al. (2023) show that the EI incurs weaker stepsize restriction when compared with EM scheme. Other works have derived its convergence in Wasserstein distance (Cheng et al., 2018), KL divergence (Ma et al., 2021) and Rényi divergence (Zhang et al., 2023). Other discretization schemes are proposed in Shen and Lee (2019); Li et al. (2019); He et al. (2020); Foster et al. (2021); Monmarché (2021); Foster et al. (2022); Johnston et al. (2023), whose convergence guarantee are obtained in Wasserstein distance without achieving better dependence on terms such as the smoothness and LSI constants. In this work, we show that EI can be applied to discretize both MULD and N-ULD to achieve fast convergence.

2.3 Definitions and assumptions

For each method considered, we study their behavior in settings where the minimizing distribution satisfies a Log-Sobolev inequality.

Definition 1 (LSI). *A measure $\pi \in \mathcal{P}_2(\mathbb{R}^d)$ satisfies Log-Sobolev Inequality (LSI) with parameter $\mathscr{C}_{LSI} > 0$, if for any $\rho \in \mathcal{P}_2(\mathbb{R}^d)$*

$$\mathsf{KL}(\rho\|\pi) \leq \frac{1}{2\mathscr{C}_{LSI}}\mathsf{FI}(\rho\|\pi). \tag{5}$$

We also work with the following distribution $\hat{\mu} \in \mathcal{P}_2(\mathbb{R}^{2d})$ that appears in the Fokker-Planck equation (28) of MULD (see Appendix A.3). Note that the limiting distribution $\mu_* \in \mathcal{P}_2(\mathbb{R}^{2d})$ of MULD satisfies $\mu_* = \hat{\mu}_*$.

Definition 2. *Throughout, we define the distribution $\hat{\mu}$ associated with the X-marginal of distribution μ and a functional F to be*

$$\hat{\mu}(x,v) \propto \exp\left(-\frac{\delta F}{\delta \rho}(\mu^X, x) - \frac{1}{2}\|v\|^2\right). \tag{6}$$

We also introduce the same three assumptions on F as Chen et al. (2023) for establishing the non-asymptotic convergence of the MULD and N-ULD.

Assumption 2.1 (Convexity). *F is convex in the linear sense, which means for any $\rho_1, \rho_2 \in \mathcal{P}_2(\mathbb{R}^d)$ and $t \in [0,1]$ the functional satisfies*

$$F(t\rho_1 + (1-t)\rho_2) \leq tF(\rho_1) + (1-t)F(\rho_2). \tag{7}$$

Assumption 2.2 ($\mathscr{L}$-smoothness). *F is smooth, which means the intrinsic derivative exists and for any $\rho_1, \rho_2 \in \mathcal{P}_2(\mathbb{R}^d)$, $x_1, x_2 \in \mathbb{R}^d$ and some $1 \leq \mathscr{L} < \infty$ satisfies*

$$\|D_\rho F(\rho_1, x_1) - D_\rho F(\rho_2, x_2)\| \leq \mathscr{L}(W_1(\rho_1, \rho_2) + \|x_1 - x_2\|). \tag{8}$$

Assumption 2.3 (LSI). *The distribution (6) satisfies LSI with constant $0 < \mathscr{C}_{LSI} \leq 1$ for any $\mu \in \mathcal{P}_2(\mathbb{R}^d)$.*

The X-marginal of distribution (6), which is related to the optimization gap, was first utilized by Nitanda et al. (2022) to establish convergence of MLD. Note that if $\hat{\mu}^X(x) \propto \exp(-\frac{\delta F}{\delta \rho}(\mu^X, x))$ satisfies LSI for any $\mu \in \mathcal{P}_2(\mathbb{R}^{2d})$ with constant $\tau > 0$, then Assumption 2.3 is satisfied with the choice $\mathscr{C}_{LSI} = \min\{1/2, \tau\}$. We refer our readers to Chen et al. (2022, 2023); Suzuki et al. (2023) for the verification of Assumptions 2.1 and 2.3 in a variety of settings. Suzuki et al. (2023) consider a weaker smoothness assumption than Assumption 2.2 where they use W_2 distance in place of W_1 distance. They verify smoothness in W_2 distance for three examples including training mean-field neural networks, MMD minimization and KSD minimization, whereas Chen et al. (2022) verify smoothness in W_1 distance only for the example of training mean-field neural networks. In this paper, we verify $\mathscr{L}$-smoothness in W_1 distance (Assumption 2.2) for the other two examples (see Section C.1). Beyond Assumptions 2.1-2.3, we introduce four additional assumptions that are sufficient for our spacetime discretization analysis.

Assumption 2.4 (Bounded Gradient). *For any $\rho \in \mathcal{P}_2(\mathbb{R}^d)$, the intrinsic derivative of F satisfies (where $\mathscr{L} > 0$)*

$$\|D_\rho F(\rho, x)\| \leq \mathscr{L}(1 + \|x\|). \tag{9}$$

Notably, Suzuki et al. (2023) assume that F can be decomposed as $F(\rho) = U(\rho) + \mathbb{E}_{x\sim\rho}[r(x)]$ where $\|D_\rho U(\rho, x)\| \leq R$ for any $\rho \in \mathcal{P}(\mathbb{R}^d)$, $x \in \mathbb{R}^d$, and where $r(x)$ is a differentiable function satisfying $\|\nabla r(x) - \nabla r(y)\| \leq \lambda_2\|x - y\|$ with $\nabla r(0) = 0$ in order to establish the convergence of their spacetime discretization of MLD. Thus, their assumption that $\|D_\rho F(\rho, x)\| \leq \|D_\rho U(\rho, x)\| +$

$\|\nabla r(x)\| \leq R + \lambda_2 \|x\|$ implies Assumption 2.4 holds with the choice $\mathscr{L} \geq \max\{R, \lambda_2\}$. The next three assumptions are needed for bounding the second moment of the iterates $(x_t, v_t)_{t \geq 0}$ and $(x_t^i, v_t^i)_{t \geq 0}$ along MULD and N-ULD, which is crucial for the establishment of our discrete-time convergence.

Assumption 2.5. *For all $\mu \in \mathcal{P}_2(\mathbb{R}^{2d})$, the distribution (6) given F satisfies $\mathbb{E}_{\hat{\mu}} \| \cdot \|^2 \lesssim d$.*

Assumption 2.6. *Given the initial distribution $\mu_0 \in \mathcal{P}_2(\mathbb{R}^{2d})$ of the discrete-time process of MULD, functional F and satisfies $F(\mu_0^X) \lesssim \mathscr{L} d$.*

Assumption 2.7. *Given the initial distribution $\mu_0^N \in \mathcal{P}_2(\mathbb{R}^{2Nd})$ of the discrete-spacetime process of MULD, functional F satisfies $\mathbb{E}_{\boldsymbol{x}_0 \sim (\mu_0^X)^N} F(\mu_{\boldsymbol{x}_0}) \lesssim \mathscr{L} d$, where μ_0^N is the N-tensor product of μ_0 and $\mu_{\boldsymbol{x}_0} = \frac{1}{N} \sum_{i=1}^N \delta_{x_0^i}$ with $x_0^i \sim \mu_0^X$.*

While Assumptions 2.5-2.7 are sufficient, they may not be necessary for the iterates to be bounded. Nevertheless, we argue these assumptions are not too restrictive by verifying them for three examples introduced above including training mean-field neural networks, MMD minimization and KSD minimization in Section 4.

2.4 Related work

Techniques for establishing the continuous-time convergence of the mean-field underdamped systems and their space-discretization (N-particle systems) are centered around *coupling* and *hypocoercivity*. The latter one is also known as functional approaches (Villani, 2009). The coupling approach generally constructs a joint probability of the mean-field and N-particle systems to make the analytic comparison between them. Based on coupling approaches, Guillin et al. (2022); Bolley et al. (2010); Bou-Rabee and Schuh (2023) show convergence of the underdamped dynamics with mean-field interaction and its space-discretization. Duong and Tugaut (2018); Kazeykina et al. (2020) study the ergodicity of the MULD without a quantitative rate. Under the setting of small mean-field dependence, Kazeykina et al. (2020) show exponential contraction using coupling techniques in Eberle et al. (2019a,b). The functional approach (hypocoercivity) generally constructs appropriate Lyapunov functionals and studies how their values change along the dynamics. Based on hypocoercivity, Monmarché (2017); Guillin et al. (2021); Guillin and Monmarché (2021); Bayraktar et al. (2022) establish the exponential convergence of the mean-field underdamped systems and its propagation of chaos by constructing a suitable Lyapunov functional. Nevertheless, most of the works above only consider specific settings of MULD such as singular interactions and two-body interactions, which restricts the application to real-world problems. Setting $\gamma = 1$, Chen et al. (2023) establish the exponential convergence of MULD and N-ULD using the hypocoercivity technique in Villani (2009). Under Assumptions 2.1-2.3, they derive the convergence without restricting the size of interactions, which subsumes many settings above. Notably, the techniques of our Theorems 3.1 and 3.2 are adopted from Chen et al. (2023) based on hypocoercivity where we consider other choices of γ to improve the decaying rate of MULD and N-ULD established in Chen et al. (2023).

3 N-particle underdamped Langevin algorithm

Our first step is to establish the global convergence of the *mean-field underdamped Langevin algorithm* (MULA),

$$\mathrm{d}x_t = v_t \mathrm{d}t, \qquad\qquad\qquad\qquad (\text{MULA})$$

$$\mathrm{d}v_t = -\gamma v_t \mathrm{d}t - D_\rho F(\mu_{kh}^X, x_{kh}) \mathrm{d}t + \sqrt{2\gamma} \mathrm{d}B_t,$$

for stepsize h, $t \in [kh, (k+1)h]$ and $k = 1, ..., K$. Note that MULA is the EI time-discretization of the MULD, where each step will now require integrating from $t = kh$ to $t = (k+1)h$ for stepsize h. MULA is intractable to implement in most instances given we do not often have access to μ_{kh}^X per iteration. This prompts us to consider the particle approximation which uses $\mu_{\mathbf{x}_{kh}} = \frac{1}{N} \sum_{i=1}^{N} \delta_{x_{kh}^i}$ to approximate μ_{kh}^X where $(x_k^i)_{i=1}^N$ are iid samples from μ_k^X:

$$
\begin{aligned}
\mathrm{d}x_t^i &= v_t^i \mathrm{d}t, \\
\mathrm{d}v_t^i &= -\gamma v_t^i \mathrm{d}t - D_\rho F(\mu_{\mathbf{x}_{kh}}, x_{kh}^i)\mathrm{d}t + \sqrt{2\gamma}\mathrm{d}\mathrm{B}_t^i,
\end{aligned}
\tag{11}
$$

for stepsize h, $t \in [kh, (k+1)h]$, $i = 1, ..., N$, $k \in \mathbb{N}$ and $\mu_{\mathbf{x}_{kh}} = \frac{1}{N} \sum_{i=1}^{N} \delta_{x_{kh}^i}$. Integrating the particle system (11) from $t = kh$ to $t = (k+1)h$ for stepsize h and $i = 1, ..., N$, we obtain our proposed Algorithm 1 which we refer to as the *N-particle underdamped Langevin algorithm* (N-ULA).

Algorithm 1 N-particle underdamped Langevin algorithm (NULA)

Require: F satisfies Assumptions 2.1-2.5 and 2.7
1: Initialize $\mathbf{x}_0 = (x_0^1, ..., x_0^N)$, $\mathbf{v}_0 = (v_0^1, ..., v_0^N)$, h, γ
   Specify φ_0, φ_1, φ_2, Σ_{11}, Σ_{12}, Σ_{22} using (35) and (36).
2: **for** $k = 0, ..., K - 1$ **do**
3:   **for** $i = 1, ..., N$ **do**
4:   $\begin{bmatrix} (\mathrm{B}_k^i)^x \\ (\mathrm{B}_k^i)^v \end{bmatrix} \sim \mathcal{N}\left(0, \begin{bmatrix} \Sigma^{11} I_d & \Sigma^{12} I_d \\ \Sigma^{12} I_d & \Sigma^{22} I_d \end{bmatrix} \right)$
5:   $x_{k+1}^i = x_k^i + \varphi_0\, v_k^i - \varphi_1\, D_\mu F(\mu_{\mathbf{x}_k}, x_k^i) + (\mathrm{B}_k^i)^x$
6:   $v_{k+1}^i = \varphi_2\, v_k^i - \varphi_0\, D_\mu F(\mu_{\mathbf{x}_k}, x_k^i) + (\mathrm{B}_k^i)^v$
7:   **end for**
8: **end for**
9: **return** $(x_K^1, ..., x_K^N)$

The update parameters of Algorithm 1, φ_0, φ_1, φ_2 and Σ_{11}, Σ_{12}, Σ_{22}, are functions of γ and stepsize h. Thus, we need to specify the value of γ and h to compute the update parameters and initialize $(\mathbf{x}_0, \mathbf{v}_0) \sim \mu_0^N \in \mathcal{P}_2(\mathbb{R}^{2Nd})$ before running the algorithm.

3.1 Convergence analysis

We begin by leveraging entropic hypocoercivity and Theorems 2.1 and 2.2 from Chen et al. (2023) to analyze the continuous-time dynamics MULD and N-ULD. Let

$$
S = \begin{pmatrix} 1/\mathscr{L} & 1/\sqrt{\mathscr{L}} \\ 1/\sqrt{\mathscr{L}} & 2 \end{pmatrix} \otimes I_d.
\tag{12}
$$

We construct the Lyapunov functional similar to Chen et al. (2023), but with a different choice of S. Theorem 3.1 is established by showing the following functional is decaying along the trajectory of MULD.

$$
\mathcal{E}(\mu) := \mathcal{F}(\mu) + \mathsf{FI}_S(\mu \| \hat{\mu}), \text{ where}
\tag{13}
$$

$$
\mathcal{F}(\mu) := F(\mu^X) + \int \frac{1}{2}\|v\|^2 \mu(\mathrm{d}x\mathrm{d}v) + \mathrm{Ent}(\mu).
$$

Our second Theorem 3.2 establishes the convergence of N-ULD. Denote $\mathbf{x} = (x^1, ..., x^N)$, $\mathbf{v} = (v^1, ..., v^N)$, $\mu^N = \mathrm{Law}(\mathbf{x}, \mathbf{v})$, and μ_*^N as the limiting distribution of N-ULD satisfying $\mu_*^N(\mathbf{x}, \mathbf{v}) \propto$

$\exp\left(-NF(\mu_{\mathbf{x}}) - \frac{1}{2}\|\mathbf{v}\|^2\right)$ (see the derivation of limiting distribution in Appendix A.4). Denote $\nabla_i := (\nabla_{x^i}, \nabla_{v^i})^\mathsf{T}$. We obtain our guarantee by showing the functional is decaying along the trajectory of N-ULD:

$$\mathcal{E}^N(\mu^N) := \mathcal{F}^N(\mu^N) + \mathsf{FI}_S^N(\mu^N\|\mu_*^N), \text{ where} \tag{14}$$

$$\mathsf{FI}_S^N(\mu^N\|\mu_*^N) := \sum_{i=1}^N \mathbb{E}_{\mu^N}\left\|S^{1/2}\nabla_i \log \frac{\mu^N}{\mu_*^N}\right\|^2, \text{ and}$$

$$\mathcal{F}^N(\mu^N) := \int NF(\mu_{\mathbf{x}}) + \frac{1}{2}\|\mathbf{v}\|^2 \mu^N(\mathrm{d}\mathbf{x}\mathrm{d}\mathbf{v}) + \mathrm{Ent}(\mu^N).$$

Theorem 3.1 (Mean-field underdamped Langevin dynamics). *If Assumptions 2.1-2.3 hold, μ_0 has finite second moment, finite entropy and finite Fisher information, then the law μ_t of the MULD with $\gamma = \sqrt{\mathscr{L}}$ and $\mathcal{E}$ defined in (13) satisfy,*

$$\mathcal{F}(\mu_t) - \mathcal{F}(\mu_*) \leq (\mathcal{E}(\mu_0) - \mathcal{E}(\mu_*)) \exp\left(-\frac{\mathscr{C}_{\mathsf{LSI}}}{3\sqrt{\mathscr{L}}}t\right).$$

Theorem 3.2 (N-particle underdamped Langevin dynamics). *If Assumptions 2.1-2.3 hold, μ_0^N has finite second moment, finite entropy, finite Fisher information, and $N \geq (\mathscr{L}/\mathscr{C}_{\mathsf{LSI}})(32 + 24\mathscr{L}/\mathscr{C}_{\mathsf{LSI}})$, then the joint law μ_t^N of the N-ULD with $\gamma = \sqrt{\mathscr{L}}$ and $\mathcal{E}^N$ defined in (14) satisfy*

$$\frac{1}{N}\mathcal{F}^N(\mu_t^N) - \mathcal{F}(\mu_*) \leq \frac{\mathcal{E}_0^N}{N}\exp\left(-\frac{\mathscr{C}_{\mathsf{LSI}}}{6\sqrt{\mathscr{L}}}t\right) + \frac{\mathcal{B}}{N},$$

where $\mathcal{B} = \frac{60\mathscr{L}d}{\mathscr{C}_{\mathsf{LSI}}} + \frac{36\mathscr{L}^2 d}{\mathscr{C}_{\mathsf{LSI}}^2}$, $\mathcal{E}_0^N := \mathcal{E}^N(\mu_0^N) - N\mathcal{E}(\mu_*)$.

Note that $\mathcal{E}_0^N = \mathcal{F}^N(\mu_0^N) - N\mathcal{F}(\mu_*) + \mathsf{FI}_S^N(\mu_0^N\|\mu_*^N) \geq 0$ by Lemma 4. The decaying rate given in Theorem 3.1 resembles the decaying rate of ULD in Zhang et al. (2023) with similar choices of γ and S. Theorem 3.2 implies the non-uniform-in-N convergence of N-ULD, which incorporates a bias term involving N due to the particle approximation. Our proof technique is more refined but parallel to that of Chen et al. (2023) where our faster convergence and smaller bias is achieved by choosing $\gamma = \sqrt{\mathscr{L}}$ instead of $\gamma = 1$ (see Table 1).

Our main results analyze the convergence of the discrete-time processes MULA and N-ULA as well as their mixing time guarantees to generate an ϵ-approximate solution in TV distance with the specific choice of initialization, damping coefficient γ, and stepsize h.

Theorem 3.3 (Mean-field underdamped Langevin algorithm). *In addition to the assumptions specified in Theorems 3.1, let Assumptions 2.4-2.6 hold. Denote $\bar{\mu}_K$ the law of (x_K, v_K) of the MULA and $\kappa := \mathscr{L}/\mathscr{C}_{\mathsf{LSI}}$. Then in order to ensure $\|\bar{\mu}_K - \mu_*\|_{\mathsf{TV}} \leq \epsilon$, it suffices to choose $\gamma = \sqrt{\mathscr{L}}$, $\bar{\mu}_0 = \mathcal{N}(0, I_{2d})$, and*

$$h = \widetilde{\Theta}\left(\frac{\mathscr{C}_{\mathsf{LSI}}\epsilon}{\mathscr{L}^{3/2}d^{1/2}}\right), \quad K = \widetilde{\Theta}\left(\frac{\kappa^2 d^{1/2}}{\epsilon}\right).$$

A similar guarantee can be stated for the N-particle system (11) with the additional requirement that the number of particles scale according to the dimension of the problem and problem parameters.

Discretization	Method	# of particles	Mixing time
Time-discretizations	MLA (Nitanda et al., 2022)	*	$\widetilde{\Theta}\left(\kappa^2\mathscr{L}d/\epsilon^2\right)$
	EI-ULMC (Zhang et al., 2023)	*	$\widetilde{\Theta}\left(\kappa^{3/2}d^{1/2}/\epsilon\right)$
	MULA (Ours)	*	$\widetilde{\Theta}\left(\kappa^2 d^{1/2}/\epsilon\right)$
Space-discretizations	N-ULD (Chen et al. (2023))	$\Theta\left(\kappa^2\mathscr{L}d/\epsilon^2\right)$	$\widetilde{\Theta}\left(\kappa\right)$
	N-ULD (Ours)	$\Theta\left(\kappa^2 d/\epsilon^2\right)$	$\widetilde{\Theta}\left(\kappa/\mathscr{L}^{1/2}\right)$
spacetime discretizations	N-LA (Suzuki et al., 2023)	$\Theta\left(\kappa\mathscr{L}^3 d/\epsilon^2\right)$	$\widetilde{\Theta}\left(\kappa^2\mathscr{L}d/\epsilon^2\right)$
	NULA (Ours)	$\Theta\left(\kappa^2 d/\epsilon^2\right)$	$\widetilde{\Theta}\left(\kappa^2 d^{1/2}/\epsilon\right)$

Table 1: Comparison of algorithms in terms of the mixing time and number of particles to achieve ϵ-approximate solutions in TV distance. $\kappa := \mathscr{L}/\mathscr{C}_{\mathsf{LSI}}$. * represents that we do not need particle approximation for this method.

Theorem 3.4 (N-particle underdamped Langevin algorithm). *In addition to the assumptions specified in Theorem 3.2, let Assumptions 2.4, 2.5 and 2.7 hold. Denote $\bar{\mu}_K^i$ the law of (x_K^i, v_K^i) of the NULA for $i = 1,...,N$ and $\kappa := \mathscr{L}/\mathscr{C}_{\mathsf{LSI}}$. Then in order to ensure $\frac{1}{N}\sum_{i=1}^N \|\bar{\mu}_K^i - \mu_*\|_{\mathsf{TV}} \le \epsilon$, it suffices to choose $\gamma = \sqrt{\mathscr{L}}$, $\bar{\mu}_0^N = \mathcal{N}(0, I_{2Nd})$,*

$$h = \widetilde{\Theta}\left(\frac{\mathscr{C}_{\mathsf{LSI}}\epsilon}{\mathscr{L}^{3/2}d^{1/2}}\right), \ K = \widetilde{\Theta}\left(\frac{\kappa^2 d^{1/2}}{\epsilon}\right),$$

and the number of particles $N = \Theta\left(\kappa^2 d/\epsilon^2\right)$.

3.2 Proof sketches

For the continuous-time results, we outline the proof of Theorem 3.1 (and analogously Theorem 3.2) in this section to provide intuition for how choosing $\gamma = \sqrt{\mathscr{L}}$ can improve the decaying rate of MULD. We begin with a review of some notations of hypocoercivity in Villani (2009); Chen et al. (2023):

$$A_t = \nabla_v, \ C_t = \nabla_x, \ Y_t = \left(\|A_t u_t\|_{L^2(\mu_t)}, \|A_t^2 u_t\|_{L^2(\mu_t)}, \|C_t u_t\|_{L^2(\mu_t)}, \|C_t A_t u_t\|_{L^2(\mu_t)}\right)^{\mathsf{T}},$$

where $u_t = \log\frac{\mu_t}{\hat{\mu}_t}$. Inheriting the analysis of Theorem 2.1 in Chen et al. (2023) and Lemma 32 in Villani (2009), we show that for a general γ, the Lyapunov functional (13) with $S = [s_{ij}] \otimes I_d \in \mathbb{R}^{2d\times 2d}$ is decreasing along MULD satisfying

$$\frac{\mathrm{d}}{\mathrm{d}t}\mathcal{E}(\mu_t) \le -Y_t^{\mathsf{T}}\mathcal{K}Y_t, \tag{15}$$

where $s_{11} = c$, $s_{12} = s_{21} = b$, $s_{22} = a$ and $\mathcal{K}$ is an upper triangle matrix with diagonal elements $(\gamma+2\gamma a-4\mathscr{L}b, 2\gamma a, 2b, 2\gamma c)$. To ensure $S \succ 0$ and the right hand side of (15) negative, the criteria of choosing positive constants a, b, c should be $ac > b^2$ and $\mathcal{K} \succ 0$. If we specify $\gamma = 1$, we can choose $a = c = 2\mathscr{L}$ and $b = 1$ satisfying the criteria. Then we obtain $\lambda_{\mathsf{min}}(\mathcal{K}) = 1$ and

$$\frac{\mathrm{d}}{\mathrm{d}t}\mathcal{E}(\mu_t) \le -\lambda_{\mathsf{min}}(\mathcal{K})Y_t^{\mathsf{T}}Y_t \le -\mathscr{C}_{\mathsf{LSI}}(\mathcal{F}(\mu_t) - \mathcal{F}(\mu_*)) - \frac{1}{2\lambda_{\mathsf{max}}(S)}\mathsf{FI}_S(\mu_t\|\hat{\mu}_t)$$

$$\le -\frac{\mathscr{C}_{\mathsf{LSI}}}{6\mathscr{L}}(\mathcal{E}(\mu_t) - \mathcal{E}(\mu_*))$$

Applying Grönwall's inequality leads to the decaying rate $O(\mathscr{C}_{\mathsf{LSI}}/\mathscr{L})$ of MULD ($\gamma = 1$) in Chen et al. (2023). If we specify $\gamma = \sqrt{\mathscr{L}}$, we can choose $b = 1/\sqrt{\mathscr{L}}$, $a = 2$, $c = 1/\mathscr{L}$ satisfying the criteria. Then we obtain $\lambda_{\min}(\mathcal{K}) = 2/\sqrt{\mathscr{L}}$ and

$$\frac{\mathrm{d}}{\mathrm{d}t}\mathcal{E}(\mu_t) \leq -\lambda_{\min}(\mathcal{K})Y_t^\mathsf{T}Y_t \leq -\frac{2\mathscr{C}_{\mathsf{LSI}}}{\sqrt{\mathscr{L}}}(\mathcal{F}(\mu_t) - \mathcal{F}(\mu_*)) - \frac{1}{\lambda_{\max}(S)\sqrt{\mathscr{L}}}\mathsf{FI}_S(\mu_t\|\hat{\mu}_t)$$

$$\leq -\frac{\mathscr{C}_{\mathsf{LSI}}}{3\sqrt{\mathscr{L}}}(\mathcal{E}(\mu_t) - \mathcal{E}(\mu_*))$$

Applying Grönwall's inequality leads to the improved decaying rate $O(\mathscr{C}_{\mathsf{LSI}}/\sqrt{\mathscr{L}})$ of MULD ($\gamma = \sqrt{\mathscr{L}}$) in our Theorem 3.1. We defer the whole proof to Appendix D.

For discretization errors, we outline the proof of Theorem 3.3 (and analogously Theorem 3.4) in this section. Let $(\mu_t)_{t\geq 0}$ and $(\bar{\mu}_{t/h})_{t\geq 0}$ represent the law of MULD and MULA initialized at μ_0. Let $\mathbf{Q}_{kh}$ and $\mathbf{P}_{kh}$ denote probability measures of MULD and MULA on the space of paths $C([0,kh], \mathbb{R}^{2d})$. Invoking Girsanov's theorem (Girsanov, 1960; Kutoyants, 2004; Le Gall, 2016) and Assumption 2.2, we can upper bound the pathwise divergence between MULD and MULA in KL divergence for stepsize h and $k = 1, ..., K$ under Assumptions 2.2 and 2.4:

$$\mathsf{KL}(\mathbf{Q}_{Kh}\|\mathbf{P}_{Kh}) \lesssim \frac{\mathscr{L}^4h^5}{\gamma}\sum_{k=0}^{K-1}\mathbb{E}_{\mathbf{Q}_{Kh}}\|x_{kh}\|^2 + \frac{\mathscr{L}^2h^3}{\gamma}\sum_{k=0}^{K-1}\mathbb{E}_{\mathbf{Q}_{Kh}}\|v_{kh}\|^2 + \frac{\mathscr{L}^4h^5K}{\gamma} + \mathscr{L}^2h^4Kd \quad (16)$$

The derivation of (16) is similar to that of Zhang et al. (2023); they establish the discretization error of EI-ULMC in q-th order Rényi divergence ($q \in [1, 2)$), which has KL divergence as a special case ($q = 1$). Their smoothness assumption on the potential function V is $(\mathscr{L}, s)$-weak smoothness, which recovers $\mathscr{L}$-smoothness when $s = 1$. We use many similar techniques of bounding the discretization error to those of Zhang et al. (2023). Their Lemma 26 can be generalized to our Lemma 7 in the mean-field setting, which describes an intermediate process of deriving (16). Applying the data processing inequality, we can upper bound the KL divergence between the time marginal laws of the iterates by KL divergence between path measures:

$$\mathsf{KL}(\mu_T\|\bar{\mu}_K) \leq \mathsf{KL}(\mathbf{Q}_{Kh}\|\mathbf{P}_{Kh}),$$

where $T = Kh$. Uniformly upper bounding the right-hand side of (16) requires obtaining uniform bounds for $\mathbb{E}_{\mathbf{Q}_{Kh}}\|x_{kh}\|^2$ and $\mathbb{E}_{\mathbf{Q}_{Kh}}\|v_{kh}\|^2$; If we were to rely on existing techniques Zhang et al. (2023), we would need a χ^2-convergence guarantee of MULD. Given χ^2-convergence is not established for MULD by previous works, we develop different techniques to uniformly upper bound the iterates of MULD and N-ULD. More specifically, we have

$$\mathbb{E}_{\mathbf{Q}_T}\|(x_t, v_t)\|^2 = W_2^2(\mu_t, \delta_0) \lesssim \underbrace{W_2^2(\mu_t, \mu_*)}_{\mathsf{I}} + \underbrace{W_2^2(\mu_*, \delta_0)}_{\mathsf{II}}, \ t \in [0, T],$$

where δ_0 is Dirac measure on $\mathsf{0} \in \mathbb{R}^{2d}$, and II is the second moment of μ_* denoted by $\mathbf{m}_2^2$. Now we need to upper bound I. Under Assumption 2.3, μ_* satisfies LSI implying Talagrand's inequality: $\mathsf{I} \lesssim \mathsf{KL}(\mu_t\|\mu_*)/\mathscr{C}_{\mathsf{LSI}}$. Under Assumptions 2.1 and 2.2, Lemma 4.2 in Chen et al. (2023) establishes the following relation between KL divergence and energy gap:

$$\mathsf{KL}(\mu_t\|\mu_*) \leq \mathcal{F}(\mu_t) - \mathcal{F}(\mu_*). \quad (17)$$

Moreover, Kazeykina et al. (2020); Chen et al. (2023) demonstrate that $\mathcal{F}(\mu_t)$ is decreasing along MULD. According to two conclusions above, I can be bounded as

$$\mathsf{I} \lesssim \frac{\mathsf{KL}(\mu_t\|\mu_*)}{\mathscr{C}_{\mathsf{LSI}}} \leq \frac{\mathcal{F}(\mu_t) - \mathcal{F}(\mu_*)}{\mathscr{C}_{\mathsf{LSI}}} \leq \frac{\mathcal{F}(\mu_0) - \mathcal{F}(\mu_*)}{\mathscr{C}_{\mathsf{LSI}}} \leq \frac{\mathcal{F}(\mu_0)}{\mathscr{C}_{\mathsf{LSI}}},$$

where the last inequality follows from the assumption that $\mathcal{F}(\mu_*) \geq 0$. Therefore, under Assumptions 2.5 on $\mathbf{m}_2^2$ and 2.6 on $F(\mu_0)$, our Lemma 8 establishes the upper bound of $\mathbb{E}_{\mathbf{Q}_T}\|(x_t, v_t)\|^2$ in terms of $\mathscr{L}$, $\mathscr{C}_{\mathsf{LSI}}$ and d, which implies the uniform upper bound of $\mathsf{KL}(\mu_T\|\bar{\mu}_K)$. Applying Pinsker's inequality

$$\|\bar{\mu}_K - \mu_T\|_{\mathsf{TV}} \lesssim \sqrt{\mathsf{KL}(\mu_T\|\bar{\mu}_K)},$$

we can convert the discretization error bound in KL divergence to that in TV distance. Combining Pinsker's inequality and relation (17), we derive the continuous-time convergence of MULD in Theorem 3.1 in TV distance:

$$\|\mu_T - \mu_*\|_{\mathsf{TV}} \lesssim \sqrt{\mathsf{KL}(\mu_T\|\mu_*)} \leq \sqrt{\mathcal{F}(\mu_T) - \mathcal{F}(\mu_*)}. \tag{18}$$

Applying the triangle inequality to $\|\bar{\mu}_K - \mu_*\|_{\mathsf{TV}}$, the TV distance between the law of MULA at Kh and the limiting distribution of MULD, we obtain the global convergence of MULA:

$$\|\bar{\mu}_K - \mu_*\|_{\mathsf{TV}} \leq \underbrace{\|\bar{\mu}_K - \mu_T\|_{\mathsf{TV}}}_{\mathcal{B}} + \underbrace{\|\mu_T - \mu_*\|_{\mathsf{TV}}}_{\mathcal{V}},$$

where $\mathcal{V}$ vanishes exponentially fast as $T \to \infty$ and $\mathcal{B}$ is a vanishing bias as $h \to 0$. To ensure $\mathcal{V} + \mathcal{B} \leq \epsilon$, it suffices to choose $T = \widetilde{\Theta}(\sqrt{\mathscr{L}}/\mathscr{C}_{\mathsf{LSI}})$ and specify h, K as in Theorem 3.3. The whole proof is deferred to Appendix E.

3.3 Discussion of mixing time results

We summarize the convergence results of MULA, NULA and several existing methods including EI-ULMC, the EM-discretization of MLD (referred to as MLA (Nitanda et al., 2022)), and its finite-particle system (referred to as N-LA (Suzuki et al., 2023)) in Table 1. For the mixing time to generate an ϵ-approximate solution in TV distance, our proposed MULA and N-ULA achieve better dependence on $\mathscr{L}$, d and ϵ than MLA and N-LA, and keep the same dependence on $\mathscr{C}_{\mathsf{LSI}}$ as MLA and N-LA, which justifies that our methods are fast. For the number of particles, we improve the dependence on $\mathscr{L}$ for N-ULD ($\gamma = \sqrt{\mathscr{L}}$) when compared with N-ULD ($\gamma = 1$) in Chen et al. (2023) and for N-ULA when compared with N-LA. Particularly, our dependence on the smoothness constant in the number of particle guarantee of N-ULA is $\Theta(\mathscr{L}^2)$ whereas the counterpart of N-LA is $\Theta(\mathscr{L}^4)$. However, our dependence on the LSI constant in the number of particle guarantee of N-ULA is $\Theta(\mathscr{C}_{\mathsf{LSI}}^{-2})$ whereas the counterpart of N-LA is $\Theta(\mathscr{C}_{\mathsf{LSI}}^{-1})$.

Note that Nitanda et al. (2022) consider MLA in the neural network setting where they specifically choose F to be the objective (19) and propose assumptions on l, h and r. Suzuki et al. (2023) consider N-LA in a setting where they specify that $F(\mu) = U(\mu) + \mathbb{E}_\mu[r(x)]$ and propose assumptions on U and r. Consequently, they use different notations of the smoothness constant and establish the convergence rate in energy gap $\mathcal{F}(\bar{\mu}_K) - \mathcal{F}(\mu_*)$ instead of the TV distance. To make a fair comparison, we equivalently translate those smoothness constants into $\mathscr{L}$ and convert convergence rates of MLA and N-LA to those in TV distance by relation (17) and Pinsker's inequality (see Appendix G).

4 Applications of Algorithm 1

In this section, we will show how Algorithm 1 can be applied to several applications by verifying Assumptions 2.1-2.7 hold for these examples. We present these results in full details in Appendix C.

4.1 Training mean-field neural networks

Consider a two-layer mean-field neural network (with infinite depth), which can be parameterized as $h(\rho; a) := \mathbb{E}_{x \sim \rho}[h(x; a)]$, where $h(x; a)$ represents a single neuron with trainable parameter x and input a (e.g. $h(x; a) = \sigma(x^\mathsf{T} a)$ for activation function σ); ρ is the probability distribution of the parameter x. Given dataset $(a_i, b_i)_{i=1}^n$ and loss function ℓ, we choose F in objective (2) to be

$$F(\mu^X) = \frac{1}{n} \sum_{i=1}^n \ell(h(\mu^X; a_i), b_i) + \frac{\lambda'}{2} \mathbb{E}_{x \sim \mu^X} \|x\|^2, \tag{19}$$

The objectives (19) satisfy Assumptions 2.1-2.4 for specific common choices ℓ and h described in several works (Nitanda et al., 2022; Chen et al., 2022, 2023; Suzuki et al., 2023). If there exists $\mathscr{L} > 0$ such that the activation function satisfies $|h(x; a)| \leq \sqrt{\mathscr{L}}$ (also proposed in Suzuki et al. (2023)) and the convex loss function ℓ is quadratic or satisfies $|\partial_1 \ell| \leq \sqrt{\mathscr{L}}$ (also proposed in Nitanda et al. (2022)), F satisfies Assumption 2.5 with $\lambda' \leq (2\pi)^3 \exp(-8\mathscr{L})$. Finally, if in addition we assume ℓ is $\sqrt{\mathscr{L}}$-Lipschitz and choose $\lambda' \leq (2\pi)^3 \exp(-8\mathscr{L})$, $\mu_0 = \mathcal{N}(0, I_{2d})$ and $\mu_0^N = \mathcal{N}(0, I_{2Nd})$, Assumptions 2.6 and 2.7 will be satisfied.

4.2 Density estimation via MMD minimization

The maximum mean discrepancy between two probability measures ρ and π is defined as $\mathcal{M}(\rho \| \pi) = \iint [k(x, x) - 2k(x, y) + k(y, y)] d\rho(x) d\pi(y)$, where k is a positive definite kernel. Similar to Example 2 in Suzuki et al. (2023), we consider the non-parametric density estimation using the Gaussian mixture model, which can be parameterized as $p(\rho; z) := \mathbb{E}_{x \sim \rho}[p(x; z)]$, where $p(x; z)$ is the Gaussian density function of z with mean x and a user-specified variance σ^2. Given a set of samples $\{z_i\}_{i=1}^n$ from the target distribution p^*, our goal is to fit p^* by minimizing the empirical version of $\mathcal{M}(p(\rho; z) \| p^*)$, defined as

$$\hat{\mathcal{M}}(\rho) = \iiint p(x; z) p(x'; z') k(z, z') dz dz' d\rho(x) d\rho(x') - 2 \int \left(\frac{1}{n} \sum_{i=1}^n \int p(x; z) k(z, z_i) dz \right) d\rho(x).$$

We choose F in objective (2) to be

$$F(\mu^X) = \hat{\mathcal{M}}(\mu^X) + \frac{\lambda'}{2} \mathbb{E}_{x \sim \mu^X} \|x\|^2, \tag{20}$$

where $\lambda' > 0$. Suzuki et al. (2023) show that objective (20) satisfies Assumptions 2.1, 2.3 and 2.4 by choosing a smooth and light-tailed kernel k, such as Gaussian radial basis function (RBF) kernel defined as $k(z, z') := \exp(-\|z - z'\|^2 / 2\sigma'^2)$ for $\sigma' > 0$. We also verify that objective (20) also satisfies our Assumption 2.2 with the same choice of kernel. With Gaussian RBF kernel k ($\sigma' = \sigma$), we provide verification in Appendix C that objective (20) satisfies Assumptions 2.5-2.7 when $\lambda' \leq 3\pi/25$, $\mu_0 = \mathcal{N}(0, I_{2d})$ and $\mu_0^N = \mathcal{N}(0, I_{2Nd})$.

4.3 Kernel Stein discrepancy minimization

Kernel Stein discrepancy (KSD) minimization is a method for sampling from a target distribution ρ_* if we have the access to the score function $s_{\rho_*}(x) = \nabla \log \rho_*(x)$ (Chwialkowski et al., 2016; Liu et al., 2016). For a positive definite kernel k, the Stein kernel is defined as

$$u_{\rho_*}(x, x') = s_{\rho_*}^\mathsf{T}(x) k(x, x') s_{\rho_*}(x') + s_{\rho_*}^\mathsf{T}(x) \nabla_{x'} k(x, x') + \nabla_x^\mathsf{T} k(x, x') s_{\rho_*}(x') + \mathsf{tr}(\nabla_{x,x'} k(x, x')).$$

The KSD between ρ and ρ_* is defined as $\mathsf{KSD}(\rho) = \iint u_{\rho_*}(x, x')\mathrm{d}\rho(x)\mathrm{d}\rho(x')$. We choose F in (2) to be

$$F(\mu^X) = \mathsf{KSD}(\mu^X) + \frac{\lambda'}{2}\mathbb{E}_{x \sim \mu^X}\|x\|^2, \tag{21}$$

where $\lambda' > 0$. Suzuki et al. (2023) show that objective (21) satisfies Assumptions 2.1, 2.3 and 2.4 by choosing light-tailed kernel and assume the score function satisfies

$$\max_{k=1,2,3}\{\|\nabla^{\otimes k}\log\rho_*(x)\|_{\mathsf{op}}\} \leq \mathscr{L}(1 + \|x\|). \tag{22}$$

More specifically, if $\mu_* \propto \exp(-V)$, the potential function V should satisfies

$$\max_{k=1,2,3}\{\|\nabla^{\otimes k}\nabla V(x)\|_{\mathsf{op}}\} \leq \mathscr{L}(1 + \|x\|),$$

which subsumes many distributions. Choosing the same kernel as in Suzuki et al. (2023), we verify in Appendix C that (21) also satisfies Assumption 2.2 and satisfies our Assumptions 2.5-2.7 with $\lambda' \leq \min\{(2\pi)^3\exp(-4\mathscr{L}), \mathscr{L}, d\}$, $\mu_0 = \mathcal{N}(0, I_{2d})$ and $\mu_0^N = \mathcal{N}(0, I_{2Nd})$.

5 Numerical experiments

We verify our theoretical findings by providing empirical support in this section. Our experiment[1] is to approximate a Gaussian function $f(z) = \exp(-\|z - m\|^2/2d)$ for $z \in \mathbb{R}^d$ and unknown $m \in \mathbb{R}^d$ by a mean-field two-layer neural network with tanh activation. Consider the empirical risk minimization problem (19) with quadratic loss function ℓ, $d = 10^3$, $\lambda' = 10^{-4}$ and n randomly generated data samples from $f(z)$ ($n = 100$), described by

$$F(\rho) = \frac{1}{2n}\sum_{i=1}^{n}(h(\mu; a_i) - f(a_i))^2 + \frac{\lambda'}{2}\mathbb{E}_{x \sim \rho}[\|x\|^2].$$

F satisfy Assumptions 2.1-2.7 with the choice of ℓ, h, and thus we apply Algorithm 1 for minimizing the objective above. Note that the number of neurons in the first hidden layer is equivalent to the number of particles in N-ULA, and we choose $N \in \{256, 512, 1024, 2048\}$. The intrinsic derivative of F for the j-th particle in our method is given by

$$D_\rho F(\mu_{\mathbf{x}}, x^j) = \frac{1}{n}\sum_{i=1}^{n}(\frac{1}{N}\sum_{s=1}^{N}h(x^s; a_i) - f(a_i))\nabla h(x^j; a_i) + \lambda' x^j.$$

Note that $\frac{1}{N}\sum_{s=1}^{N}h(x_s; a)$ is in fact a two-layer neural network with N neurons. Instead of fine-tuning γ and stepsize h in N-ULA, we directly fine-tune the value of φ_0, φ_1 and φ_2 in Algorithm 1 by grid search. For simplifying the computation, we approximate $(\mathrm{B}_k^i)^x$ and $(\mathrm{B}_k^i)^v$ by $\eta\xi_k^x$ and $\eta\xi_k^v$ where ξ_k^x and ξ_k^v are independent standard Gaussian, and then we fine-tune the scaling scalar η. We compare our method (N-ULA) to N-LA with stepsize h_1 and scaling scalar λ_1 given by,

$$x_{k+1}^j = x_k^j - h_1 D_\rho F(\mu_{\mathbf{x}_k}, x_k^j) + \sqrt{2\lambda_1 h_1}\xi_k^i \tag{N-LA}$$

for $i = 1, ..., N$, $k = 1, ..., K$ and $\xi_k^i \sim \mathcal{N}(0, I_d)$, and EM-UNLA (the EM discretization of the N-ULD with stepsize h_2 and scaling scalar λ_2) whose update is given by

$$\begin{aligned}x_{k+1}^j &= x_k^j + h_2 v_k^j \\ v_{k+1}^j &= (1 - \gamma h_2)v_k^j - h_2 D_\rho F(\mu_{\mathbf{x}_k}, x_k^j) + \sqrt{2\lambda_2 h_2}\xi_k^i\end{aligned} \tag{EM-N-ULA}$$

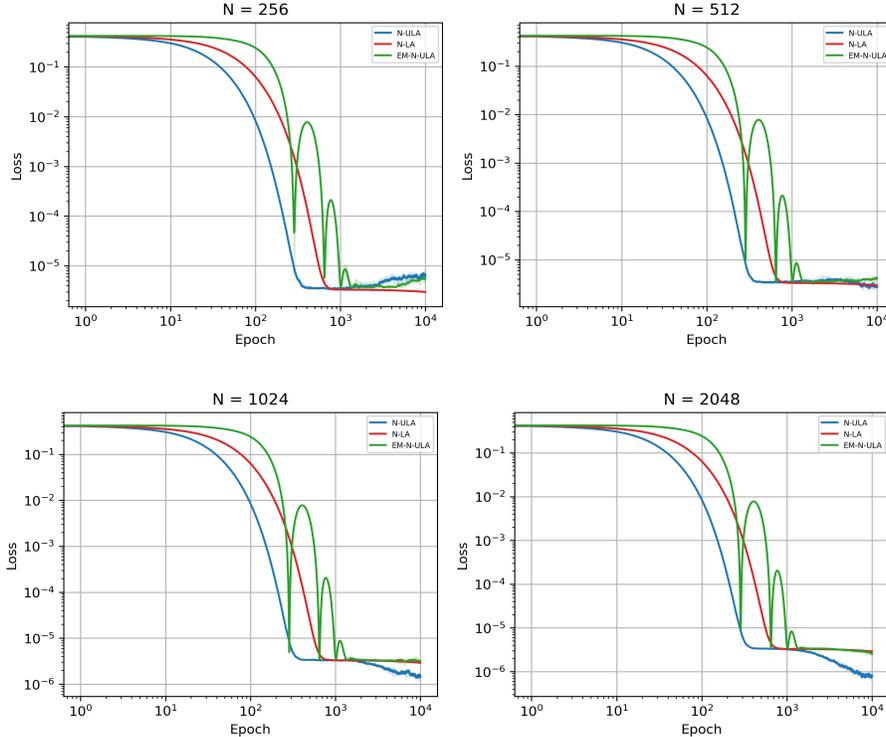[1]Code for our experiments can be found at `https://github.com/QiangFu09/NULA`.

Figure 1: Evaluation on N-ULA, N-LA and EM-N-ULA with different number of particles N where x-axis represents the training epochs and y-axis represents the value of $\frac{1}{2n}\sum_{i=1}^{n}(\frac{1}{N}\sum_{s=1}^{N}h(x^s;a_i) - f(a_i))^2$. Our method often enjoys better performance in the high particle-approximation regime which is consistent with our theoretical findings.

for $i = 1, ..., N$, $k = 1, ..., K$ and $\xi_k^i \sim \mathcal{N}(0, I_d)$ in the same task. We choose $K = 10^4$ and also fine-tune h_1, λ_1 and h_2, λ_2 to make fair comparison. We postpone our choice of hyperparameters to the Appendix F. For each algorithm in our experiment, we initialize $x_0^j \sim \mathcal{N}(0, 10^{-2}I_d)$ and $v_0^j \sim \mathcal{N}(0, 10^{-2}I_d)$ for $j = 1, ..., N$, average 5 runs over random seeds in $\{0, 1, 2, 3, 4\}$ and generate the error bars by filling between the largest and the smallest value per iteration. Fig. 1 illustrates the effectiveness of N-ULA. For each N, N-ULA enjoys faster convergence than N-LA and EM-N-ULA. Notably, there is an interesting phenomenon in our experiments. For $N = 256$, both N-ULA and EM-N-ULA suffer from convergence instability, which means that the loss will escape the stable convergence regime and slightly go up after many training epochs. However, N-ULA outperforms N-LA and EM-N-ULA without convergence instability for $N = 512, 1024, 2048$, and the loss of N-ULA even goes on decreasing when the losses of N-LA and EM-N-ULA keep stable for $N = 1024, 2048$. This phenomenon matches our theory that we do not reduce the number of particles for N-ULA when compared with N-LA (see Table 1). These observations suggest that our method performs better in the high particle-approximation regime. Fig. 2 demonstrates this finding more transparently. The second row of Fig. 1 also suggests that EM discretization incurs a larger bias than EI.

6   Discussion

To summarize, this paper (1) improves the convergence guarantees in Chen et al. (2023) with a refined Lyapunov analysis (Theorems 3.1 and 3.2); (2) discretizes the MULD and N-ULD with a
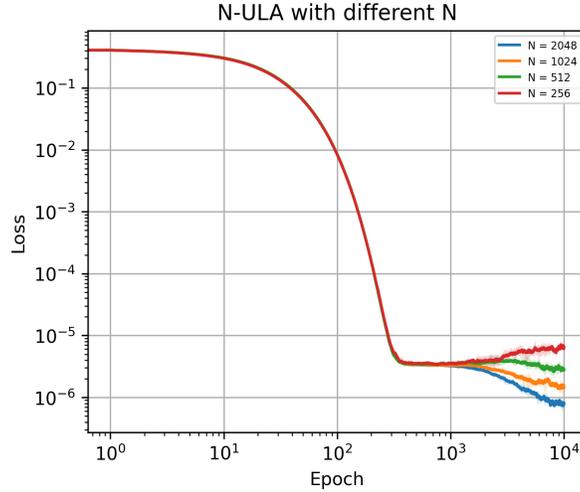
Figure 2: NULA with different number of particles

scheme which results in smaller bias than the EM scheme; and (3) presents a novel discretization analysis of MULD and N-ULD. We also verify that these methods work when the objective is W_1 smooth. We now note several directions for future potential developments. First, it is unclear what the optimal choice of damping coefficient γ is for MULD and N-ULD. Understanding whether the optimal choice has been found is of interest. Second, we obtain convergence rates for the MULA and N-ULA in TV distance, which are not consistent with the convergence rates of MULD, N-ULD, MLA and N-LA in energy gap (e.g. $\mathcal{F}(\mu_t) - \mathcal{F}(\mu_*)$). We hope to establish our results in the energy gap or KL divergence in the future. What's more, our techniques on uniformly bounding the iterates of MULD and N-ULD combined with Assumptions 2.5-2.7 generates an additional $\mathscr{C}_{\mathsf{LSI}}$ after using Talagrand's inequality, which leads to non-improvement of $\mathscr{C}_{\mathsf{LSI}}$ for MULA and N-ULA. We hope to explore whether it is possible to weaken those assumptions and refine the analysis of uniformly bounding the iterates to improve the dependence of $\mathscr{C}_{\mathsf{LSI}}$ in the mixing time and number of particles of MULA and N-ULA.

References

Michael Arbel, Anna Korba, Adil Salim, and Arthur Gretton. Maximum mean discrepancy gradient flow. *Advances in Neural Information Processing Systems*, 32, 2019.

Erhan Bayraktar, Qi Feng, and Wuchen Li. Exponential entropy dissipation for weakly self-consistent vlasov-fokker-planck equations. *arXiv preprint arXiv:2204.12049*, 2022.

François Bolley, Arnaud Guillin, and Florent Malrieu. Trend to equilibrium and particle approximation for a weakly selfconsistent vlasov-fokker-planck equation. *ESAIM: Mathematical Modelling and Numerical Analysis*, 44(5):867–884, 2010.

Nawaf Bou-Rabee and Katharina Schuh. Convergence of unadjusted hamiltonian monte carlo for mean-field models. *Electronic Journal of Probability*, 28:1–40, 2023.

Yu Cao, Jianfeng Lu, and Lihan Wang. On explicit l 2-convergence rate estimate for underdamped langevin dynamics. *Archive for Rational Mechanics and Analysis*, 247(5):90, 2023.

Fan Chen, Zhenjie Ren, and Songbo Wang. Uniform-in-time propagation of chaos for mean field langevin dynamics. *arXiv preprint arXiv:2212.03050*, 2022.

Fan Chen, Yiqing Lin, Zhenjie Ren, and Songbo Wang. Uniform-in-time propagation of chaos for kinetic mean field langevin dynamics. *arXiv preprint arXiv:2307.02168*, 2023.

Xiang Cheng, Niladri S Chatterji, Peter L Bartlett, and Michael I Jordan. Underdamped langevin mcmc: A non-asymptotic analysis. In *Conference on learning theory*, pages 300–323. PMLR, 2018.

Lénaïc Chizat. Mean-field langevin dynamics: Exponential convergence and annealing. *arXiv preprint arXiv:2202.01009*, 2022.

Kacper Chwialkowski, Heiko Strathmann, and Arthur Gretton. A kernel test of goodness of fit. In *International conference on machine learning*, pages 2606–2615. PMLR, 2016.

Julien Claisse, Giovanni Conforti, Zhenjie Ren, and Songbo Wang. Mean field optimization problem regularized by fisher information. *arXiv preprint arXiv:2302.05938*, 2023.

Manh Hong Duong and Julian Tugaut. The vlasov-fokker-planck equation in non-convex landscapes: convergence to equilibrium. 2018.

Andreas Eberle, Arnaud Guillin, and Raphael Zimmer. Couplings and quantitative contraction rates for langevin dynamics. 2019a.

Andreas Eberle, Arnaud Guillin, and Raphael Zimmer. Quantitative harris-type theorems for diffusions and mckean–vlasov processes. *Transactions of the American Mathematical Society*, 371 (10):7135–7173, 2019b.

James Foster, Terry Lyons, and Harald Oberhauser. The shifted ode method for underdamped langevin mcmc. *arXiv preprint arXiv:2101.03446*, 2021.

James Foster, Goncalo dos Reis, and Calum Strange. High order splitting methods for sdes satisfying a commutativity condition. *arXiv preprint arXiv:2210.17543*, 2022.

Qiang Fu, Dongchu Xu, and Ashia Camage Wilson. Accelerated stochastic optimization methods under quasar-convexity. In *International Conference on Machine Learning*, pages 10431–10460. PMLR, 2023.

Igor Vladimirovich Girsanov. On transforming a certain class of stochastic processes by absolutely continuous substitution of measures. *Theory of Probability & Its Applications*, 5(3):285–301, 1960.

Arthur Gretton, Karsten Borgwardt, Malte Rasch, Bernhard Schölkopf, and Alex Smola. A kernel method for the two-sample-problem. *Advances in neural information processing systems*, 19, 2006.

Arnaud Guillin and Pierre Monmarché. Uniform long-time and propagation of chaos estimates for mean field kinetic particles in non-convex landscapes. *Journal of Statistical Physics*, 185:1–20, 2021.

Arnaud Guillin, Wei Liu, Liming Wu, and Chaoen Zhang. The kinetic fokker-planck equation with mean field interaction. *Journal de Mathématiques Pures et Appliquées*, 150:1–23, 2021.

Arnaud Guillin, Pierre Le Bris, and Pierre Monmarché. Convergence rates for the vlasov-fokker-planck equation and uniform in time propagation of chaos in non convex cases. *Electronic Journal of Probability*, 27:1–44, 2022.

Ye He, Krishnakumar Balasubramanian, and Murat A Erdogdu. On the ergodicity, bias and asymptotic normality of randomized midpoint sampling method. *Advances in Neural Information Processing Systems*, 33:7366–7376, 2020.

Oliver Hinder, Aaron Sidford, and Nimit Sohoni. Near-optimal methods for minimizing star-convex functions and beyond. In *Conference on learning theory*, pages 1894–1938. PMLR, 2020.

Lars Hörmander. Hypoelliptic second order differential equations. 1967.

Kaitong Hu, Zhenjie Ren, David Siska, and Lukasz Szpruch. Mean-field langevin dynamics and energy landscape of neural networks. *arXiv preprint arXiv:1905.07769*, 2019.

Tim Johnston, Iosif Lytras, and Sotirios Sabanis. Kinetic langevin mcmc sampling without gradient lipschitz continuity–the strongly convex case. *arXiv preprint arXiv:2301.08039*, 2023.

Anna Kazeykina, Zhenjie Ren, Xiaolu Tan, and Junjian Yang. Ergodicity of the underdamped mean-field langevin dynamics. *arXiv preprint arXiv:2007.14660*, 2020.

Diederik P Kingma and Jimmy Ba. Adam: A method for stochastic optimization. *arXiv preprint arXiv:1412.6980*, 2014.

Peter E Kloeden, Eckhard Platen, Matthias Gelbrich, and Werner Romisch. Numerical solution of stochastic differential equations. *SIAM Review*, 37(2):272–274, 1995.

Andrey Kolmogoroff. Zufallige bewegungen (zur theorie der brownschen bewegung). *The Annals of Mathematics*, 35(1):116, 1934.

Yu A Kutoyants. *Statistical inference for ergodic diffusion processes*. Springer Science & Business Media, 2004.

Maxime Laborde and Adam Oberman. A lyapunov analysis for accelerated gradient methods: From deterministic to stochastic case. In *International Conference on Artificial Intelligence and Statistics*, pages 602–612. PMLR, 2020.

Jean-François Le Gall. *Brownian motion, martingales, and stochastic calculus*. Springer, 2016.

Benedict Leimkuhler, Daniel Paulin, and Peter A Whalley. Contraction and convergence rates for discretized kinetic langevin dynamics. *arXiv preprint arXiv:2302.10684*, 2023.

Xuechen Li, Yi Wu, Lester Mackey, and Murat A Erdogdu. Stochastic runge-kutta accelerates langevin monte carlo and beyond. *Advances in neural information processing systems*, 32, 2019.

Qiang Liu, Jason Lee, and Michael Jordan. A kernelized stein discrepancy for goodness-of-fit tests. In *International conference on machine learning*, pages 276–284. PMLR, 2016.

Yi-An Ma, Niladri S Chatterji, Xiang Cheng, Nicolas Flammarion, Peter L Bartlett, and Michael I Jordan. Is there an analog of nesterov acceleration for gradient-based mcmc? 2021.

Song Mei, Andrea Montanari, and Phan-Minh Nguyen. A mean field view of the landscape of two-layer neural networks. *Proceedings of the National Academy of Sciences*, 115(33):E7665–E7671, 2018.

Pierre Monmarché. Long-time behaviour and propagation of chaos for mean field kinetic particles. *Stochastic Processes and their Applications*, 127(6):1721–1737, 2017.

Pierre Monmarché. High-dimensional mcmc with a standard splitting scheme for the underdamped langevin diffusion. *Electronic Journal of Statistics*, 15(2):4117–4166, 2021.

Yurii Evgen'evich Nesterov. A method of solving a convex programming problem with convergence rate o\bigl(k^2\bigr). In *Doklady Akademii Nauk*, volume 269, pages 543–547. Russian Academy of Sciences, 1983.

Atsushi Nitanda, Denny Wu, and Taiji Suzuki. Convex analysis of the mean field langevin dynamics. In *International Conference on Artificial Intelligence and Statistics*, pages 9741–9757. PMLR, 2022.

Eckhard Platen and Nicola Bruti-Liberati. *Numerical solution of stochastic differential equations with jumps in finance*, volume 64. Springer Science & Business Media, 2010.

Sebastian Ruder. An overview of gradient descent optimization algorithms. *arXiv preprint arXiv:1609.04747*, 2016.

Ruoqi Shen and Yin Tat Lee. The randomized midpoint method for log-concave sampling. *Advances in Neural Information Processing Systems*, 32, 2019.

Ilya Sutskever, James Martens, George Dahl, and Geoffrey Hinton. On the importance of initialization and momentum in deep learning. In *International conference on machine learning*, pages 1139–1147. PMLR, 2013.

Taiji Suzuki, Denny Wu, and Atsushi Nitanda. Convergence of mean-field langevin dynamics: Time and space discretization, stochastic gradient, and variance reduction. *arXiv preprint arXiv:2306.07221*, 2023.

Santosh Vempala and Andre Wibisono. Rapid convergence of the unadjusted langevin algorithm: Isoperimetry suffices. *Advances in neural information processing systems*, 32, 2019.

Cédric Villani. Limites hydrodynamiques de l'équation de boltzmann. *Séminaire Bourbaki*, 2000: 365–405, 2001.

Cédric Villani. *Hypocoercivity*, volume 202. American Mathematical Society, 2009.

Ashia C Wilson, Benjamin Recht, and Michael I Jordan. A lyapunov analysis of momentum methods in optimization. *arXiv preprint arXiv:1611.02635*, 2016.

Matthew Zhang, Sinho Chewi, Mufan Bill Li, Krishnakumar Balasubramanian, and Murat A Erdogdu. Improved discretization analysis for underdamped langevin monte carlo. *arXiv preprint arXiv:2302.08049*, 2023.

A Supplementary background

A.1 Mean-field Langevin dynamics

The law $(\rho_t)_{t \geq 0}$ of MLD solves the following non-linear Fokker-Planck equation:

$$\frac{\partial \rho_t}{\partial t} = \nabla \cdot (\rho_t D_\rho F(\rho_t, \cdot)) + \Delta \rho_t = \nabla \cdot \left(\rho_t \nabla \log \frac{\rho_t}{\hat{\rho}_t} \right), \tag{23}$$

where $\hat{\rho}_t(x) \propto \exp\left(-\frac{\delta F}{\delta \rho}(\rho_t, x)\right)$. Let $E(\rho) := F(\rho) + \mathrm{Ent}(\rho)$. The optimality condition of the EMO problem is

$$\frac{\delta E}{\delta \rho} = \frac{\delta F}{\delta \rho} + \log \rho + c = 0, \tag{24}$$

where c is a constant. Given the condition (24), the solution of EMO problem ρ_* satisfies $\rho_*(x) = \hat{\rho}_*(x) \propto \exp\left(-\frac{\delta F}{\delta \rho}(\rho_*, x)\right)$, which solves $\nabla \cdot \left(\rho_t \nabla \log \frac{\rho_t}{\hat{\rho}_t} \right) = 0$. Thus we conclude that MLD converges to the minimizer of EMO objective.

A.2 N-particle Langevin dynamics

The space-discretization of MLD is referred to as the *N-particle Langevin dynamics*,

$$\mathrm{d}x_t^i = -D_\rho F(\rho_{\mathbf{x}_t}, x_t^i)\mathrm{d}t + \sqrt{2}\mathrm{dB}_t, \tag{N-LD}$$

where $\rho_{\mathbf{x}_t} = \frac{1}{N} \sum_{i=1}^N \delta_{x_t^i}$. Let ρ_t^i denotes the law of x_t^i and ρ_t^N denotes the joint law of $\mathbf{x}_t := (x_t^1, ..., x_t^N)$. The joint law $(\rho_t^N)_{t \geq 0}$ of N-LD solves the following linear Fokker-Planck equation:

$$\frac{\partial \rho_t^N}{\partial t} = \sum_{i=1}^N \nabla_i \cdot \left(\rho_t^N D_\rho F(\rho_{\mathbf{x}_t}, x_t^i) \right) + \Delta_i \rho_t^N = \sum_{i=1}^N \nabla_i \cdot \left(\rho_t^N \nabla_i \log \frac{\rho_t^N}{\rho_*^N} \right), \tag{25}$$

where $\nabla_i := \nabla_{x^i}$, $\Delta_i := \Delta_{x^i}$ and $\rho_*^N(\mathbf{x}) \propto \exp(-NF(\rho_{\mathbf{x}}))$. Define the *N-particle free energy*:

$$E^N(\rho^N) = N \int F(\rho_{\mathbf{x}})\rho^N(\mathrm{d}x) + \mathrm{Ent}(\rho^N). \tag{26}$$

The optimality condition of minimizing the N-particle free energy (26) over $\mathcal{P}_2(\mathbb{R}^{Nd})$ is

$$\frac{\delta E^N}{\delta \rho^N} = NF(\rho_{\mathbf{x}}) + \log \rho^N + c = 0, \tag{27}$$

where c is a constant. Given the optimality condition (27), the minimizer of (26) satisfies $\rho_*^N(x) \propto \exp(-NF(\rho_{\mathbf{x}}))$, which is exactly the limiting distribution of N-LD according to (25). Thus we conclude that N-LD converges to the minimizer of (26).

A.3 Mean-field underdamped Langevin dynamics

The law $(\mu_t)_{t \geq 0}$ of MULD solves the following non-linear Fokker-Planck equation:

$$\begin{aligned} \frac{\partial \mu_t}{\partial t} &= \gamma \Delta_v \mu_t + \gamma \nabla_v \cdot (\mu_t v_t) - v \cdot \nabla_x \mu_t + D_\rho F(\mu_t^x, x_t) \cdot \nabla_v \mu_t \\ &= \nabla \cdot \left(\mu_t J_\gamma \nabla \log \frac{\mu_t}{\hat{\mu}_t} \right), \end{aligned} \tag{28}$$

where $J_\gamma = \begin{pmatrix} 0 & 1 \\ -1 & \gamma \end{pmatrix}$, $\nabla := (\nabla_x, \nabla_v)^\mathsf{T}$ and $\hat\mu_t(x, v) \propto \exp\left(-\frac{\delta F}{\delta \rho}(\mu_t^X, x) - \frac{1}{2}\|v\|^2\right)$. The optimality condition of the augmented EMO problem is

$$\frac{\delta \mathcal{F}}{\delta \mu} = \frac{\delta F}{\delta \mu} + \log \mu + \frac{1}{2}\|v\|^2 + c = 0, \tag{29}$$

where $\mathcal{F}$ is defined in (13) and c is a constant. Note that $\frac{\delta F(\mu^X)}{\delta \mu} = \frac{\delta F(\mu^X)}{\delta \rho}$. Given the optimality condition (29), the solution of the augmented EMO problem satisfies $\mu_*(x, v) = \hat\mu_*(x, v) \propto \exp\left(-\frac{\delta F}{\delta \rho}(\mu_*^X, x) - \frac{1}{2}\|v\|^2\right)$, which solves $\nabla \cdot \left(\mu_t J_\gamma \nabla \log \frac{\mu_t}{\hat\mu_t}\right) = 0$. Thus we conclude that MULD converges to the minimizer of the augmented EMO objective.

A.4 N-particle underdamped Langevin dynamics

The law $(\mu_t^N)_{t \geq 0}$ of N-ULD solves the following linear Fokker-Planck equation:

$$\frac{\partial \mu_t^N}{\partial t} = \sum_{i=1}^N \left(\gamma \Delta_{v^i} \mu_t^N + \gamma \nabla_{v^i} \cdot (\mu_t^N v_t^i) - v_t^i \cdot \nabla_{x^i} \mu_t^N + D_\rho F(\mu_{\mathbf{x}_t}, x_t^i) \cdot \nabla_{v^i} \mu_t^N\right)$$
$$= \sum_{i=1}^N \nabla_i \cdot \left(\mu_t^N J_\gamma \nabla_i \log \frac{\mu_t^N}{\hat\mu_*^N}\right), \tag{30}$$

where $J_\gamma = \begin{pmatrix} 0 & 1 \\ -1 & \gamma \end{pmatrix}$, $\nabla_i := (\nabla_{x^i}, \nabla_{v^i})^\mathsf{T}$ and $\hat\mu_*^N(x, v) \propto \exp\left(-NF(\mu_\mathbf{x}) - \frac{1}{2}\|v\|^2\right)$. Define the N-particle free energy:

$$\mathcal{F}^N(\mu^N) = \int NF(\mu_\mathbf{x}) + \frac{1}{2}\|\mathbf{v}\|^2 \mu^N(\mathrm{d}\mathbf{x}\mathrm{d}\mathbf{v}) + \mathrm{Ent}(\mu^N). \tag{31}$$

The optimality condition of minimizing the N-particle free energy (31) over $\mathcal{P}_2(\mathbb{R}^{2Nd})$ is

$$\frac{\delta \mathcal{F}^N}{\delta \mu^N} = NF(\mu_\mathbf{x}) + \frac{1}{2}\|\mathbf{v}\|^2 + \log \mu^N + c = 0, \tag{32}$$

where c is a constant. Given the optimality condition (32), the minimizer of (31) satisfies $\mu_*^N(x) \propto \exp(-NF(\mu_\mathbf{x}) - \frac{1}{2}\|\mathbf{v}\|^2)$, which is exactly the limiting distribution of N-ULD according to (30). Thus we conclude that N-ULD converges to the minimizer of (31).

B Helpful lemmas

Lemma 1. *The solution (x_t, v_t) to the discrete-time process (MULA) for $t \in [kh, (k+1)h]$ is*

$$x_t = x_{kh} + \frac{1 - e^{-\gamma(t-kh)}}{\gamma} v_{kh} - \frac{\gamma h - (1 - e^{-\gamma(t-kh)})}{\gamma^2} D_\rho F(\mu_{kh}^X, x_{kh}) + \mathrm{B}_{kh}^x,$$
$$v_t = e^{-\gamma(t-kh)} v_{kh} - \frac{1 - e^{-\gamma(t-kh)}}{\gamma} D_\rho F(\mu_{kh}^X, x_{kh}) + \mathrm{B}_{kh}^v, \tag{33}$$

where $(\mathrm{B}_{kh}^x, \mathrm{B}_{kh}^v) \in \mathbb{R}^{2d}$ is independent of k and has the joint distribution

$$\begin{bmatrix} \mathrm{B}_{kh}^x \\ \mathrm{B}_{kh}^v \end{bmatrix} \sim \mathcal{N}\left(0, \begin{bmatrix} \frac{2}{\gamma}\left(h - \frac{2(1-e^{-\gamma(t-kh)})}{\gamma} + \frac{1-e^{-2\gamma(t-kh)}}{2\gamma}\right) & \frac{1}{\gamma}\left(1 - 2e^{-\gamma(t-kh)} + e^{-2\gamma(t-kh)}\right) \\ * & 1 - e^{-2\gamma(t-kh)} \end{bmatrix} \otimes I_d\right)$$

The solution (x_t^i, v_t^i) to the discrete-time process (11) *for $i = 1, ..., N$ and $t \in [kh, (k+1)h]$ is*

$$
\begin{aligned}
x_t^i &= x_{kh}^i + \frac{1 - e^{-\gamma(t-kh)}}{\gamma} v_{kh}^i - \frac{\gamma h - (1 - e^{-\gamma(t-kh)})}{\gamma^2} D_\rho F(\mu_{\boldsymbol{x}_{kh}}, x_{kh}^i) + (\mathrm{B}_{kh}^i)^x, \\
v_t^i &= e^{-\gamma(t-kh)} v_{kh}^i - \frac{1 - e^{-\gamma(t-kh)}}{\gamma} D_\rho F(\mu_{\boldsymbol{x}_{kh}}, x_{kh}^i) + (\mathrm{B}_{kh}^i)^v.
\end{aligned}
\tag{34}
$$

where $((\mathrm{B}_{kh}^i)^x, (\mathrm{B}_{kh}^i)^v) \in \mathbb{R}^{2d}$ is independent of i, k and has the joint distribution

$$
\begin{bmatrix} (\mathrm{B}_{kh}^i)^x \\ (\mathrm{B}_{kh}^i)^v \end{bmatrix} \sim \mathcal{N} \left(0, \begin{bmatrix} \frac{2}{\gamma} \left(h - \frac{2(1 - e^{-\gamma(t-kh)})}{\gamma} + \frac{1 - e^{-2\gamma(t-kh)}}{2\gamma} \right) I_d & \frac{1}{\gamma} \left(1 - 2e^{-\gamma(t-kh)} + e^{-2\gamma(t-kh)} \right) I_d \\ \frac{1}{\gamma} \left(1 - 2e^{-\gamma(t-kh)} + e^{-2\gamma(t-kh)} \right) I_d & 1 - e^{-2\gamma(t-kh)} I_d \end{bmatrix} \right)
$$

Proof. The proof technique is similar to the proof of Lemmas 10 and 11 proposed in Cheng et al. (2018). $\qquad\square$

Choosing $t = (k+1)h$ for (34) generates the update parameters of Algorithm 1:

$$
\varphi_0 = \frac{1 - e^{-\gamma h}}{\gamma}, \ \ \varphi_1 = \frac{\gamma h - (1 - e^{-\gamma h})}{\gamma^2}, \ \ \varphi_2 = e^{-\gamma h};
\tag{35}
$$

$$
\Sigma_{11} = \frac{2}{\gamma} \left(h - \frac{2(1 - e^{-\gamma h})}{\gamma} + \frac{1 - e^{-2\gamma h}}{2\gamma} \right), \ \Sigma_{12} = \frac{1}{\gamma} \left(1 - 2e^{-\gamma h} + e^{-2\gamma h} \right), \ \Sigma_{22} = 1 - e^{-2\gamma h}.
\tag{36}
$$

Lemma 2. *Suppose $D_\rho F : \mathcal{P}_2(\mathbb{R}^d) \times \mathbb{R}^d \to \mathbb{R}^d$ admits a continuous first variation $\delta D_\rho F : \mathcal{P}_2(\mathbb{R}^d) \times \mathbb{R}^d \to \mathbb{R}^d$. Then, $D_\rho F$ is $\mathcal{L}$-Lipschitz with respect to W_1 distance satisfying*

$$
\|D_\rho F(\rho_1, x) - D_\rho F(\rho_2, x)\| \le \mathcal{L} W_1(\rho_1, \rho_2)
\tag{37}
$$

with $\mathcal{L} := \sup_{\rho' \in \mathcal{P}_2(\mathbb{R}^d)} \sup_{x, x' \in \mathbb{R}^d} \|D_\rho^2 F(\rho', x, x')\|_{\mathrm{op}}$

Proof. By the definition of functional derivative, we have

$$
\|D_\rho F(\rho_1, x) - D_\rho F(\rho_2, x)\| \le \int_0^1 \left\| \int \frac{\delta}{\delta\rho} D_\rho F((1-t)\rho_1 + t\rho_2, x, x')(\rho_1 - \rho_2) \mathrm{d}x' \right\| \mathrm{d}t
\tag{38}
$$

By Kantorovich duality and the definition of $\mathcal{L}$, which is the Liptschiz constant of $\frac{\delta}{\delta\rho} D_\rho F(\cdot, x)$, we obtain

$$
\left\| \int \frac{\delta}{\delta\rho} D_\rho F((1-t)\rho_1 + t\rho_2, x, x')(\rho_1 - \rho_2) \mathrm{d}x' \right\| \le \mathcal{L} W_1(\rho_1, \rho_2).
$$

Combining with (38), we complete the proof. $\qquad\square$

Lemma 3 (Mean-field Entropy Sandwich, Chen et al. 2023, Lemma 4.2). *Assume F satisfies Assumptions 2.1-2.3. Then for every $\mu \in \mathcal{P}_2(\mathbb{R}^{2d})$ we have*

$$
\mathsf{KL}(\mu\|\mu_*) \le \mathcal{F}(\mu) - \mathcal{F}(\mu_*) \le \mathsf{KL}(\mu\|\hat{\mu}) \le \left(1 + \frac{\mathcal{L}}{\mathcal{C}_{\mathsf{LSI}}} + \frac{\mathcal{L}^2}{2\mathcal{C}_{\mathsf{LSI}}^2} \right) \mathsf{KL}(\mu\|\mu_*).
\tag{39}
$$

Lemma 4 (Particle System's Entropy Inequality, Chen et al. 2023, Lemma 4.2). *Assume that F satisfies Assumption 2.1 and there exists a measure $\mu_* \in \mathcal{P}(\mathbb{R}^{2d})$ that admits the proximal Gibbs distribution $\mu_*(x, v) \propto \exp\left(-\frac{\delta F}{\delta\mu}(\mu_*^x, x) - \frac{1}{2}\|v\|^2 \right)$. Then for all $\mu^N \in \mathcal{P}(\mathbb{R}^{2dN})$, we have*

$$
\mathsf{KL}(\mu^N\|\mu_*^{\otimes N}) \le \mathcal{F}^N(\mu^N) - N\mathcal{F}(\mu_*).
\tag{40}
$$

Lemma 5 (Information Inequality). *Let $X_1, ..., X_N$ be measurable spaces, μ be a probability on the product space $X = X_1 \times ... \times X_N$ with $\mu = \mu^1 \otimes ... \otimes \mu^N$ and $\nu = \nu^1 \otimes ... \otimes \nu^N$ is a σ-finite measure. Then*

$$\sum_{i=1}^{N} \mathsf{KL}(\mu^i \| \nu^i) \leq \mathsf{KL}(\mu \| \nu). \tag{41}$$

Lemma 6 (Matrix Grönwall's Inequality, Zhang et al. 2023). *Let $x : \mathbb{R}_+ \to \mathbb{R}^d$, and $c \in \mathbb{R}^d$, $A \in \mathbb{R}^{d \times d}$, where A has non-negative entries. Suppose that the following inequality is satisfied componentwise:*

$$x(t) \leq c + \int_0^t A x(s) \mathrm{d}s, \quad \text{for all } t \geq 0.$$

Then the following inequality holds where $I_d \in \mathbb{R}^{d \times d}$ is the d-dimensional identity matrix:

$$x(t) \leq \left(A A^\dagger e^{At} - A A^\dagger + I_d \right) c.$$

Lemma 7. *Let $(x_t, v_t)_{t \geq 0}$ and $(x_t^i, v_t^i)_{t \geq 0}$ respectively denote the iterates of the MULD and N-ULD. Assume that $h \lesssim \mathscr{L}^{-1/2} \wedge \gamma^{-1}$. Under Assumption 2.2 and Assumption 2.4, for $t \in [kh, (k+1)h]$, we have*

$$\sup_{t \in [kh, (k+1)h]} \|x_t - x_{kh}\| \leq 2\mathscr{L} h^2 \|x_{kh}\| + 4h\|v_{kh}\| + 2\mathscr{L} h^2 + 2\sqrt{2\gamma} h \sup_{t \in [kh, (k+1)h]} \|\mathrm{B}_t - \mathrm{B}_{kh}\|$$

$$\sup_{t \in [kh, (k+1)h]} \|x_t^i - x_{kh}^i\| \leq 2\mathscr{L} h^2 \|x_{kh}^i\| + 4h\|v_{kh}^i\| + 2\mathscr{L} h^2 + 2\sqrt{2\gamma} h \sup_{t \in [kh, (k+1)h]} \|\mathrm{B}_t^i - \mathrm{B}_{kh}^i\|$$

for $i = 1, ..., N$.

Proof. We only prove the first relation, and the proof of the second relation is similar.

$$\|x_t - x_{kh}\| = \left\| \int_{kh}^t v_\tau \mathrm{d}\tau \right\| \leq h\|v_{kh}\| + \left\| \int_{kh}^t v_\tau - v_{kh} \mathrm{d}\tau \right\|$$

$$\leq h\|v_{kh}\| + \left\| \int_{kh}^t \int_0^\tau \gamma v_{\tau'} \mathrm{d}\tau' \mathrm{d}\tau \right\| + \left\| \int_{kh}^t \int_{kh}^\tau D_\rho F(\mu_{\tau'}^X, x_{\tau'}) \mathrm{d}\tau' \mathrm{d}\tau \right\| + \left\| \int_{kh}^t \int_{kh}^\tau \sqrt{2\gamma} \mathrm{d}\mathrm{B}_{\tau'} \mathrm{d}\tau \right\|$$

$$\leq h\|v_{kh}\| + \gamma h \left(h\|v_{kh}\| + \int_{kh}^t \|v_\tau - v_{kh}\| \mathrm{d}\tau \right) + \left\| \int_{kh}^t \int_{kh}^\tau D_\rho F(\mu_{\tau'}^X, x_{\tau'}) \mathrm{d}\tau' \mathrm{d}\tau \right\|$$

$$+ \left\| \int_{kh}^t \int_{kh}^\tau \sqrt{2\gamma} \mathrm{d}\mathrm{B}_{\tau'} \mathrm{d}\tau \right\|$$

$$\leq h\|v_{kh}\| + \gamma h \left(h\|v_{kh}\| + \int_{kh}^t \|v_\tau - v_{kh}\| \mathrm{d}\tau \right) + \mathscr{L} h \int_{kh}^t \|x_\tau - x_{kh}\| \mathrm{d}\tau + \mathscr{L} h^2 \|x_{kh}\|$$

$$+ \mathscr{L} h^2 + \sqrt{2\gamma} h \sup_{t \in [kh, (k+1)h]} \|\mathrm{B}_t - \mathrm{B}_{kh}\|$$

where the last inequality follows from Assumptions 2.2 and 2.4. Likewise for V:

$$\|v_t - v_{kh}\| = \left\| \int_{kh}^t \gamma v_\tau \mathrm{d}\tau \right\| + \left\| \int_{kh}^t D_\rho F(\mu_\tau^X, x_\tau) \mathrm{d}\tau \right\| + \left\| \int_{kh}^t \sqrt{2\gamma} \mathrm{d}\mathrm{B}_t \right\|$$

$$\leq \gamma \left(h\|v_{kh}\| + \int_{kh}^t \|v_\tau - v_{kh}\| \mathrm{d}\tau \right) + \left\| \int_{kh}^t D_\rho F(\mu_\tau^X, x_\tau) \mathrm{d}\tau \right\| + \sqrt{2\gamma} \sup_{t \in [kh, (k+1)h]} \|\mathrm{B}_t - \mathrm{B}_{kh}\|$$

$$\leq \gamma \left(h\|v_{kh}\| + \int_{kh}^t \|v_\tau - v_{kh}\| \mathrm{d}\tau \right) + \mathscr{L} \int_{kh}^t \|x_\tau - x_{kh}\| \mathrm{d}\tau + \mathscr{L} h + \mathscr{L} h \|x_{kh}\|$$

$$+ \sqrt{2\gamma} \sup_{t \in [kh, (k+1)h]} \|\mathrm{B}_t - \mathrm{B}_{kh}\|$$

where the last inequality follows from Assumptions 2.2 and 2.4. Before applying matrix form of Grönwall's inequality, let $c = c_1 + c_2$ with $c_2 = \begin{bmatrix} h\|v_{kh}\| \\ 0 \end{bmatrix}$,

$$A = \begin{bmatrix} \mathscr{L}h & \gamma h \\ \mathscr{L} & \gamma \end{bmatrix}, \quad c_1 = \begin{bmatrix} \mathscr{L}h^2\|x_{kh}\| + \gamma h^2\|v_{kh}\| + \mathscr{L}h^2 + \sqrt{2\gamma}h\sup_{t\in[kh,(k+1)h]}\|\mathrm{B}_t - \mathrm{B}_{kh}\| \\ \mathscr{L}h\|x_{kh}\| + \gamma h\|v_{kh}\| + \mathscr{L}h + \sqrt{2\gamma}\sup_{t\in[kh,(k+1)h]}\|\mathrm{B}_t - \mathrm{B}_{kh}\| \end{bmatrix}.$$

c_1 lies in the image space of A, and $\exp(A_t)c_1$ also lies in the image space of A. For the first component:

$$\sup_{t\in[kh,(k+1)h]}\|x_t - x_{kh}\| \leq h\exp\left((\mathscr{L}h + \gamma)h\right)\left(\mathscr{L}h\|x_{kh}\| + \gamma h\|v_{kh}\| + \mathscr{L}h + \sqrt{2\gamma}\sup_{t\in[kh,(k+1)h]}\|\mathrm{B}_t - \mathrm{B}_{kh}\|\right)$$

$$+ \frac{\mathscr{L}h\exp((\mathscr{L}h + \gamma)h) + \gamma}{\mathscr{L}h + \gamma}h\|v_{kh}\|$$

$$\leq 2h\left(\mathscr{L}h\|x_{kh}\| + 2\|v_{kh}\| + \mathscr{L}h + \sqrt{2\gamma}\sup_{t\in[kh,(k+1)h]}\|\mathrm{B}_t - \mathrm{B}_{kh}\|\right)$$

where the second inequality comes from choosing $h \lesssim \frac{1}{\mathscr{L}^{1/2}} \wedge \frac{1}{\gamma}$.

$$((AA^\dagger(\exp(Ah) - I) + I)c_2)_{(1)} = \frac{\mathscr{L}h\exp((\mathscr{L}h + \gamma)h) + \gamma}{\mathscr{L}h + \gamma}h\|v_{kh}\| \leq 2h\|v_{kh}\|$$

Combining relations above and Lemma 6 completes the proof. $\qquad\square$

Lemma 8. *Let $(x_t, v_t)_{t\geq 0}$ denote the iterates of the MULD with $(x_0, v_0) \sim \mu_0 = \mathcal{N}(0, I_{2d})$. Under Assumption 2.5 and Assumption 2.6, we have*

$$\mathbb{E}\|(x_t, v_t)\|^2 \lesssim \frac{\mathscr{L}d}{\mathscr{C}_{\mathsf{LSI}}} \tag{42}$$

Proof.

$$\mathbb{E}\|(x_t, v_t)\|^2 = W_2^2(\mu_t, \delta_0) \leq 2W_2^2(\mu_t, \mu_*) + 2W_2^2(\mu_*, \delta_0)$$

$$\leq \frac{2}{\mathscr{C}_{\mathsf{LSI}}}\mathsf{KL}(\mu_t\|\mu_*) + 2\mathbf{m}_2^2$$

$$\leq \frac{2}{\mathscr{C}_{\mathsf{LSI}}}(\mathcal{F}(\mu_t) - \mathcal{F}(\mu_*)) + 2\mathbf{m}_2^2$$

$$\leq \frac{2}{\mathscr{C}_{\mathsf{LSI}}}(\mathcal{F}(\mu_0) - \mathcal{F}(\mu_*)) + 2\mathbf{m}_2^2$$

$$\leq \frac{2}{\mathscr{C}_{\mathsf{LSI}}}\mathcal{F}(\mu_0) + 2\mathbf{m}_2^2$$

The second inequality follows from Talagrand's inequality which can be implied by Assumption 2.3.[2] The third inequality follows from Lemma 3. The fourth inequality follows that $\frac{\mathrm{d}}{\mathrm{d}t}\mathcal{F}(\mu_t) < 0$ along the MULD (Proof of Theorem 2.1 in Chen et al. (2023)) and the last inequality follows from the assumption that $\mathcal{F}(\mu_*) \geq 0$. By the definition of $\mathcal{F}(\mu)$, we have $\mathcal{F}(\mu_0) = F(\mu_0^x) + \int \frac{1}{2}\|v\|^2\mu_0(\mathrm{d}x\mathrm{d}v) + \mathrm{Ent}(\mu_0)$. Since $(x_0, v_0) \sim \mathcal{N}(0, I_{2d})$, we have $\int \frac{1}{2}\|v\|^2\mu_0(\mathrm{d}x\mathrm{d}v) \lesssim d$ and

$$|\mathrm{Ent}(\mu_0)| = \left|\int \mu_0\log\mu_0\right|$$

$$= \frac{d}{2}\log(2\pi) + \frac{1}{2}\mathbb{E}_{\mu_0}\|\cdot\|^2 \lesssim d.$$

---

[2]Assumption 2.3 states that the proximal Gibbs distribution satisfies the LSI. Note that μ_* also has the form of the proximal Gibbs distribution and thus satisfies LSI.

By Assumption 2.6, we have $F(\mu_0^x) \lesssim \mathscr{L}d$. By Assumption 2.5, we have $\mathbf{m}_2^2 \lesssim d$. Thus we have

$$\mathbb{E}\|(x_t, v_t)\|^2 \le \frac{2}{\mathscr{C}_{\mathsf{LSI}}} \mathcal{F}(\mu_0) + 2\mathbf{m}_2^2 \lesssim \frac{\mathscr{L}d}{\mathscr{C}_{\mathsf{LSI}}} + d$$

$\square$

Lemma 9. *Let $(x_t^i, v_t^i)_{i=1}^N$ denote the iterates of the N-ULD with $(x_0^i, v_0^i) \sim \mu_0^i = \mathcal{N}(0, I_{2d})$ for $i = 1, ..., N$ and $t \ge 0$. Under Assumption 2.5 and Assumption 2.7, we have*

$$\frac{1}{N} \sum_{i=1}^N \mathbb{E}\|(x_t^i, v_t^i)\|^2 \lesssim \frac{\mathscr{L}d}{\mathscr{C}_{\mathsf{LSI}}} \tag{43}$$

Proof.

$$\begin{aligned}
\frac{1}{N} \sum_{i=1}^N \mathbb{E}\|(x_t^i, v_t^i)\|^2 = \frac{1}{N} \sum_{i=1}^N W_2^2(\mu_t^i, \delta_0) &\le \frac{2}{N} \sum_{i=1}^N W_2^2(\mu_t^i, \mu_*) + 2W_2^2(\mu_*, \delta_0) \\
&\le \frac{2}{\mathscr{C}_{\mathsf{LSI}}} \frac{1}{N} \sum_{i=1}^N \mathsf{KL}(\mu_t^i \| \mu_*) + 2\mathbf{m}_2^2 \\
&\le \frac{2}{\mathscr{C}_{\mathsf{LSI}}} \frac{1}{N} \mathsf{KL}(\mu_t^N \| \mu_*^{\otimes N}) + 2\mathbf{m}_2^2 \\
&\le \frac{2}{\mathscr{C}_{\mathsf{LSI}}} \left(\frac{1}{N} \mathcal{F}^N(\mu_t^N) - \mathcal{F}(\mu_*) \right) + 2\mathbf{m}_2^2 \\
&\le \frac{2}{N\mathscr{C}_{\mathsf{LSI}}} \mathcal{F}^N(\mu_0^N) + 2\mathbf{m}_2^2
\end{aligned}$$

The second inequality follows from Talagrand's inequality which can be implied by Assumption 2.3. The third inequality follows from Lemma 5. The fourth inequality follows from Lemma 4 and the last inequality follows that $\frac{\mathrm{d}}{\mathrm{d}t} \mathcal{F}^N(\mu_t^N) < 0$ along the N-ULD (Proof of Theorem 2.2 in Chen et al. (2023)) and $\mathcal{F}(\mu_*) \ge 0$. By the definition of $\mathcal{F}^N(\mu^N)$, we have $\mathcal{F}^N(\mu_0^N) = \int (NF(\mu_{\mathbf{x}}) + \frac{1}{2}\|\mathbf{v}\|^2)\mu_0^N(\mathrm{d}\mathbf{x}\mathrm{d}\mathbf{v}) + \mathrm{Ent}(\mu_0^N)$. Similar to the proof of Lemma 8, since $(\mathbf{x}, \mathbf{v}) \sim \mathcal{N}(0, I_{2Nd})$, we have $\int \frac{1}{2}\|\mathbf{v}\|^2 \mu_0^N(\mathrm{d}\mathbf{x}\mathrm{d}\mathbf{v}) \lesssim Nd$ and $|\mathrm{Ent}(\mu_0^N)| \lesssim Nd$. By Assumption 2.7 and Assumption 2.5, we also have $\int NF(\mu_{\mathbf{x}})\mu_0^N(\mathrm{d}\mathbf{x}\mathrm{d}\mathbf{v}) \lesssim N\mathscr{L}d$ and $\mathbf{m}_2^2 \lesssim d$. Thus we have

$$\begin{aligned}
\frac{1}{N} \sum_{i=1}^N \mathbb{E}\|(x_t^i, v_t^i)\|^2 &\le \frac{2}{N\mathscr{C}_{\mathsf{LSI}}} \mathcal{F}^N(\mu_0^N) + 2\mathbf{m}_2^2 \\
&= \frac{2}{N\mathscr{C}_{\mathsf{LSI}}} \left(\int (NF(\mu_{\mathbf{x}}) + \frac{1}{2}\|\mathbf{v}\|^2)\mu_0^N(\mathrm{d}\mathbf{x}\mathrm{d}\mathbf{v}) + \mathrm{Ent}(\mu_0^N) \right) + 2\mathbf{m}_2^2 \\
&\lesssim \frac{1}{N\mathscr{C}_{\mathsf{LSI}}} (N\mathscr{L}d + Nd) + d \lesssim \frac{\mathscr{L}d}{\mathscr{C}_{\mathsf{LSI}}} + d
\end{aligned}$$

$\square$

Lemma 10 (Girsanov's Theorem, (Zhang et al. (2023), Theorem 19))**.** *Consider stochastic processes $(x_t)_{t\ge0}$, $(b_t^{\boldsymbol{P}})_{t\ge0}$, $(b_t^{\boldsymbol{Q}})_{t\ge0}$ adapted to the same filtration, and $\sigma \in \mathbb{R}^{d\times d}$ any constant matrix (possibly degenerate). Let $\boldsymbol{P}_T$ and $\boldsymbol{Q}$ be probability measures on the path space $C([0, T]; \mathbb{R}^d)$ such that $(x_t)_{t\ge0}$ follows*

$$\begin{aligned}
\mathrm{d}x_t &= b_t^{\boldsymbol{P}}\mathrm{d}t + \sigma \mathrm{dB}_t^{\boldsymbol{P}} \quad \text{under } \boldsymbol{P}_T, \\
\mathrm{d}x_t &= b_t^{\boldsymbol{Q}}\mathrm{d}t + \sigma \mathrm{dB}_t^{\boldsymbol{Q}} \quad \text{under } \boldsymbol{Q}_T,
\end{aligned}$$

where $\mathrm{B}^{\boldsymbol{P}}$ and $\mathrm{B}^{\boldsymbol{Q}}$ are $\boldsymbol{P}_T$-Brownian motion and $\boldsymbol{Q}_T$-Brownian motion. Suppose there exists a process $(y_t)_{t\geq 0}$ such that

$$\sigma y_t = b_t^{\boldsymbol{P}} - b_t^{\boldsymbol{Q}},$$

and

$$\mathbb{E}_{\mathbf{Q}_T} \exp\left(\frac{1}{2}\int_0^T \|y_t\|^2 \, \mathrm{d}t\right) < \infty.$$

If we define $\sigma^\dagger$ as the Moore-Penrose pseudo-inverse of σ, then we have

$$\frac{\mathrm{d}\mathbf{P}_T}{\mathrm{d}\mathbf{Q}_T} = \exp\left(\int_0^T \langle \sigma_t^\dagger(b_t^{\boldsymbol{P}_T} - b_t^{\boldsymbol{Q}_T}), \mathrm{dB}_t^{\boldsymbol{Q}_T}\rangle - \frac{1}{2}\int_0^T \|\sigma_t^\dagger(b_t^{\boldsymbol{P}_T} - b_t^{\boldsymbol{Q}_T})\|^2 \mathrm{d}t\right)$$

Besides, $(\tilde{\mathrm{B}}_t)_{t\in[0,T]}$ defined by $\mathrm{d}\tilde{\mathrm{B}}_t := \mathrm{dB}_t + \sigma_t^\dagger(b_t^Y - b_t^X)$ is a $\mathbf{P}_T$-Brownian motion.

C   Verification of assumptions

C.1   Verification of Assumption 2.2

Smoothness in W_1 distance has been verified for training mean-field neural networks in Chen et al. (2022). Thus we only verify smoothness in W_1 distance for examples of density estimation via MMD minimization and KSD minimization. Lemma 2 provides sufficient conditions for smoothness in W_1 distance. In particular, we have

$$\|D_\rho F(\rho_1, x_1) - D_\rho F(\rho_2, x_2)\| \leq \|D_\rho F(\rho_1, x_1) - D_\rho F(\rho_2, x_1)\| + \|D_\rho F(\rho_2, x_1) - D_\rho F(\rho_2, x_2)\| \quad (44)$$

Suzuki et al. (2023) verify that $\|D_\rho F(\rho_2, x_1) - D_\rho F(\rho_2, x_2)\| \leq \mathscr{L}\|x_1 - x_2\|$ for three examples mentioned above. Thus it suffices to verify (37) for the last two examples.

MMD minimization   We now prove that objective (20) satisfies Assumption 2.2 with Gaussian RBF kernel. We choose σ' in Gaussian RBF kernel k to be σ for brevity. We reformulate (20) as

$$F(\rho) = \hat{\mathcal{M}}(\rho) + \frac{\lambda'}{2}\mathbb{E}_{x\sim\rho}\|x\|^2. \quad (45)$$

According to the definition of $\hat{\mathcal{M}}$ in Section 4, the intrinsic derivative of F is

$$D_\rho F(\rho, x) = D_\rho \hat{\mathcal{M}}(\rho, x) + \frac{\lambda'}{2}\|x\|^2$$

$$= 2\iiint \nabla_x p(x; z) p(x'; z') k(z, z') \mathrm{d}z \mathrm{d}z' \mathrm{d}\rho(x') - \frac{2}{n}\sum_{i=1}^n \int \nabla_x p(x; z) k(z, z_i) \mathrm{d}z + \frac{\lambda'}{2}\|x\|^2$$

We only need to prove $D_\mu \hat{\mathcal{M}}(\mu, x)$ is smooth. The second-order intrinsic derivative $D_\rho \hat{\mathcal{M}}(\rho, x)$ is

$$D_\rho^2 \hat{\mathcal{M}}(\rho, x, x') = 2\iint \nabla_x p(x; z) \otimes \nabla_{x'} p(x'; z') k(z, z') \mathrm{d}z \mathrm{d}z'$$

$$= \frac{2}{(2\pi\sigma^2)^d \sigma^4}\iint (x - z) \otimes (x' - z') \exp\left(-\frac{\|x - z\|^2 + \|x' - z'\|^2 + \|z - z'\|^2}{2\sigma^2}\right) \mathrm{d}z \mathrm{d}z'$$

From the relation $x \cdot \exp(-x^2/2\sigma^2) \le \sigma$ for $x \ge 0$, we have

$$
\begin{aligned}
\left\| D_\rho^2 \hat{\mathcal{M}}(\rho, x, x') \right\| &\le \frac{1}{(2\pi\sigma^2)^d \sigma^4} \iint \|x - z\| \|x' - z'\| \exp\left(-\frac{\|x - z\|^2 + \|x' - z'\|^2 + \|z - z'\|^2}{2\sigma^2} \right) \mathrm{d}z \mathrm{d}z' \\
&\le \frac{1}{(2\pi\sigma^2)^d \sigma^2} \iint \exp\left(-\frac{\|z - z'\|^2}{2\sigma^2} \right) \mathrm{d}z \mathrm{d}z' = \frac{1}{(2\pi\sigma^2)^{d/2} \sigma^2}
\end{aligned}
$$

According to Lemma 2 and (44), F defined in (45) satisfies Assumption 2.2.

KSD minimization We now prove that objective (21) satisfies Assumption 2.2 with kernel

$$
k(x, x') = \exp\left(-\frac{\|x\|^2}{2\sigma_1^2} - \frac{\|x'\|^2}{2\sigma_1^2} - \frac{\|x - x'\|^2}{2\sigma_2^2} \right). \tag{46}
$$

We also assume the score function of μ_* satisfies (22). Under this assumption on score function and with this choice of kernel, Suzuki et al. (2023) show in their Appendix A that the Stein kernel u_{ρ_*} satisfies $\sup_{x,x' \in \mathbb{R}^d} \max\{|u_{\rho_*}|, \|\nabla_x u_{\rho_*}\|, \|\nabla_x \nabla_{x'} u_{\rho_*}\|_{\mathsf{op}}\} \le \mathscr{L}$. We reformulate (21) as

$$
F(\rho) = \mathsf{KSD}(\rho) + \frac{\lambda'}{2} \mathbb{E}_{x \sim \rho} \|x\|^2. \tag{47}
$$

Similarly, we only need to verify that KSD is smooth with respect to W_1 distance. The intrinsic derivative of KSD is

$$
D_\rho \mathsf{KSD}(\rho, x) = \int \nabla_x u_{\rho_*}(x, x') \mathrm{d}\rho(x').
$$

The second-order intrinsic derivative of $D_\rho \mathsf{KSD}(\rho, x)$ is

$$
D_\rho^2 \mathsf{KSD}(\rho, x, x') = \nabla_x \nabla_{x'} u_{\rho_*}(x, x')
$$

The following relation implies Assumption 2.2 by Lemma 2.

$$
\|D_\rho^2 \mathsf{KSD}(\rho, x, x')\| = \|\nabla_x \nabla_{x'} u_{\rho_*}(x, x')\| \le \mathscr{L}
$$

C.2 Verification of Assumption 2.5

Training mean-field neural networks Denote $\hat{\mu}(x, v) = \hat{\mu}^X(x) \otimes \mathcal{N}(0, I_d)$ where $\hat{\mu}^X(x) \propto \exp\left(-\frac{\delta F}{\delta \rho}(\mu^X, x) \right)$. Since the second moment of $\mathcal{N}(0, I_d)$ is $O(d)$, it suffices to ensure $\mathbb{E}_{x \sim \hat{\mu}^X} \|x\|^2 = O(d)$. We reformulate objective (19) as:

$$
F(\rho) = \frac{1}{n} \sum_{i=1}^n \ell(h(\rho; a_i), b_i) + \frac{\lambda'}{2} \mathbb{E}_{x \sim \rho}[\|x\|^2]. \tag{48}
$$

- We will prove that Assumption 2.5 holds if $|h(x; a)| \le \sqrt{\mathscr{L}}$ (such activation functions include tanh and sigmoid) and $|\partial_1 \ell| \le \sqrt{\mathscr{L}}$ (such loss functions include logistic loss, Huber loss and log-cosh loss) or ℓ is quadratic. The functional derivative of F is

$$
\frac{\delta F}{\delta \rho}(\mu^X, x) = \frac{1}{n} \sum_{i=1}^n \left[\partial_1 \ell(h(\mu^X; a_i), b_i) h(x; a_i) \right] + \frac{\lambda'}{2} \|x\|^2
$$

Consider the case where $|\partial_1 \ell| \leq \sqrt{\mathscr{L}}$. Since $|h(x;a)| \leq \sqrt{\mathscr{L}}$, we have $|\partial_1 \ell(h(\mu^X;a_i),b_i)h(x;a_i)| \leq \mathscr{L}$. Let $Z = \int \exp\left(-\frac{\delta F}{\delta \rho}(\mu^X, x)\right) \mathrm{d}x$, and we have

$$\mathbb{E}_{\hat{\mu}^X} \| \cdot \|^2 = \frac{1}{Z} \int \|x\|^2 \exp\left(-\frac{1}{n}\sum_{i=1}^{n}\left[\partial_1 \ell(h(\mu^X;a_i),b_i)h(x;a_i)\right] - \frac{\lambda'}{2}\|x\|^2\right) \mathrm{d}x := \frac{Z'}{Z} \quad (49)$$

Now we bound Z' and Z respectively.

$$Z' \leq \int \|x\|^2 \exp\left(\mathscr{L} - \frac{\lambda'}{2}\|x\|^2\right) \mathrm{d}x \lesssim \frac{\exp(\mathscr{L})d}{\lambda'},$$

$$Z \geq \int \exp\left(-\mathscr{L} - \frac{\lambda'}{2}\|x\|^2\right) \mathrm{d}x = \exp(-\mathscr{L})\left(\frac{2\pi}{\lambda'}\right)^{d/2}$$

Choose $\lambda' \leq (2\pi)^3 \exp(-4\mathscr{L})$ which implies $\lambda' \leq \frac{(2\pi)^{\frac{d}{d-2}}}{\exp\left(\frac{4\mathscr{L}}{d-2}\right)}$, and we have $\mathbb{E}_{\hat{\mu}^X}\| \cdot \|^2 = \frac{Z'}{Z} \lesssim \frac{\exp(2\mathscr{L})}{\lambda'\left(\frac{2\pi}{\lambda'}\right)^{d/2}}d \leq d$. Consider the case where ℓ is quadratic. $|h(\mu^X;a_i)| = |\int h(x;a_i)\mu^X(\mathrm{d}x)| \leq \int |h(x;a_i)|\mu(\mathrm{d}x) \leq \sqrt{\mathscr{L}}$, thus we have $|\partial_1 \ell(h(\mu^X;a_i),b_i)h(x;a_i)| = |(h(\mu^X;a_i)-b_i)h(x;a_i)| \leq \mathscr{L}+|b_i|\sqrt{\mathscr{L}}$. We can scale the label to ensure $\max_{i=1}^{n}|b_i| \leq \sqrt{\mathscr{L}}$, and we obtain $|\partial_1 \ell(h(\mu^X;a_i),b_i)h(x;a_i)| \leq 2\mathscr{L}$. The remaining proof keeps the same with $\lambda' \leq (2\pi)^3 \exp(-8\mathscr{L})$.

- We will prove that Assumption 2.5 holds if $|h(x;a)| \leq \sqrt{\mathscr{L}}(1+\|x\|)$ (such activation functions include ReLU, GeLU, Softplus, SiLU) and $|\partial_1 \ell| \leq \sqrt{\mathscr{L}}$. Under these conditions, we have $|\partial_1 \ell(h(\mu^X;a_i),b_i)h(x;a_i)| \leq \mathscr{L}(1+\|x\|)$. Then, based on (49), we obtain

$$Z' \leq \int \|x\|^2 \exp\left(\mathscr{L}(1+\|x\|) - \frac{\lambda'}{2}\|x\|^2\right) \mathrm{d}x \leq \exp(\mathscr{L})\int \|x\|^2 \exp\left(\frac{3\mathscr{L}^2}{2\lambda'} - \frac{\lambda'}{3}\|x\|^2\right) \mathrm{d}x$$

$$\lesssim \exp\left(\mathscr{L} + \frac{3\mathscr{L}^2}{2\lambda'}\right)\frac{d}{\lambda'}.$$

We also have

$$Z \geq \int \exp\left(-\mathscr{L}(1+\|x\|) - \frac{\lambda'}{2}\|x\|^2\right) \mathrm{d}x \geq \exp(\mathscr{L})\int \exp\left(-\frac{\mathscr{L}^2}{\lambda'} - \frac{3\lambda'}{4}\|x\|^2\right) \mathrm{d}x$$

$$= \exp\left(\mathscr{L} - \frac{\mathscr{L}^2}{\lambda'}\right)\left(\frac{4\pi}{3\lambda'}\right)^{d/2}$$

Combining the upper bound of Z' and the lower bound of Z, if $d \geq \frac{5\mathscr{L}^2}{\lambda'}\left(\log\frac{4\pi}{3}\right)^{-1}$, we obtain

$$\mathbb{E}_{\hat{\mu}^X}\| \cdot \|^2 = \frac{Z'}{Z} \lesssim \exp\left(\frac{5\mathscr{L}^2}{2\lambda'}\right)\frac{d}{\lambda'}\left(\frac{3\lambda'}{4\pi}\right)^{d/2} \leq \exp\left(\frac{5\mathscr{L}^2}{2\lambda'}\right)\left(\frac{3}{4\pi}\right)^{d/2}d \leq d.$$

Note that $d \geq \frac{5\mathscr{L}^2}{\lambda'}\left(\log\frac{4\pi}{3}\right)^{-1}$ is possible for large-scale problems.

MMD minimization We now prove that objective (20) satisfies Assumption 2.5 with Gaussian RBF kernel. We choose σ' in Gaussian RBF kernel k to be σ for brevity. We reformulate (20) as

$$F(\rho) = \hat{\mathcal{M}}(\rho) + \frac{\lambda'}{2}\mathbb{E}_{x \sim \rho}\|x\|^2. \quad (50)$$

According to the definition of $\hat{\mathcal{M}}(\rho)$ in Section 4, the functional derivative of $\hat{\mathcal{M}}(\rho)$ is

$$\frac{\delta \hat{\mathcal{M}}}{\delta \rho}(\rho, x) = \underbrace{2 \iiint p(x; z)p(x'; z')k(z, z')\mathrm{d}z\mathrm{d}z'\mathrm{d}\rho(x')}_{\mathsf{P}} - \underbrace{\frac{2}{n}\sum_{i=1}^{n}\int p(x; z)k(z, z_i)\mathrm{d}z}_{\mathsf{Q}} \tag{51}$$

Next we bound each part of $\frac{\delta \hat{\mathcal{M}}}{\delta \rho}(\rho, x)$. For P, we have

$$
\begin{aligned}
\frac{1}{2}\mathsf{P} &= \frac{1}{(2\pi\sigma^2)^d}\iiint \exp\left(-\frac{\|x - z\|^2}{2\sigma^2} - \frac{\|x' - z'\|^2}{2\sigma^2} - \frac{\|z - z'\|^2}{2\sigma^2}\right)\mathrm{d}z\mathrm{d}z'\mathrm{d}\rho(x') \\
&= \frac{(\pi\sigma^2)^{\frac{d}{2}}}{(2\pi\sigma^2)^d}\iint \exp\left(-\frac{\|x - x'\|^2}{6\sigma^2} - \frac{3\|z' - \frac{2}{3}x' - \frac{1}{3}x\|^2}{4\sigma^2}\right)\mathrm{d}z'\mathrm{d}\rho(x') \\
&= \left(\frac{1}{\sqrt{3}}\right)^d \int \exp\left(-\frac{\|x - x'\|^2}{6\sigma^2}\right)\mathrm{d}\rho(x') \le \left(\frac{1}{\sqrt{3}}\right)^d
\end{aligned}
$$

where the last inequality follows from the relation $\exp\left(-\frac{\|x-x'\|^2}{6\sigma^2}\right) \le 1$. For Q, we have

$$
\begin{aligned}
\frac{1}{2}\mathsf{Q} &= \frac{1}{(2\pi\sigma^2)^{\frac{d}{2}}}\frac{1}{n}\sum_{i=1}^{n}\int \exp\left(-\frac{\|x - z\|^2}{2\sigma^2} - \frac{\|z - z_i\|^2}{2\sigma^2}\right)\mathrm{d}z \\
&= \frac{1}{(2\pi\sigma^2)^{\frac{d}{2}}}\frac{1}{n}\sum_{i=1}^{n}\exp\left(-\frac{\|x\|^2 + \|z_i\|^2}{2\sigma^2} + \frac{\|z_i + x\|^2}{4\sigma^2}\right)\int \exp\left(-\frac{\|z - \frac{1}{2}z_i - \frac{1}{2}x\|^2}{\sigma^2}\right)\mathrm{d}z \\
&= \left(\frac{1}{\sqrt{2}}\right)^d\frac{1}{n}\sum_{i=1}^{n}\exp\left(-\frac{\|x\|^2 + \|z_i\|^2}{2\sigma^2} + \frac{\|z_i + x\|^2}{4\sigma^2}\right) \le \left(\frac{1}{\sqrt{2}}\right)^d
\end{aligned}
$$

where the last inequality follows from the relation $\|z_i + x\|^2 \le 2\|z_i\|^2 + 2\|x\|^2$. Note that $\mathsf{P} \ge 0$ and $\mathsf{Q} \ge 0$. Combining the bound of P and Q, we obtain the bound of $\frac{\delta \hat{\mathcal{M}}}{\delta \rho}(\rho, x)$ as follows:

$$-\sqrt{2} \le -2\left(\frac{1}{\sqrt{2}}\right)^d \le \frac{\delta \hat{\mathcal{M}}(\mu)}{\delta \mu}(x) = \mathsf{P} - \mathsf{Q} \le 2\left(\frac{1}{\sqrt{3}}\right)^d \le \sqrt{3} \tag{52}$$

Let $\hat{\mu}^X(x) = \exp\left(-\frac{\delta F}{\delta \rho}(\mu^X, x)\right)/Z$ where $Z = \int \exp\left(-\frac{\delta F}{\delta \rho}(\mu^X, x)\right)\mathrm{d}x$, and we have

$$\mathbb{E}_{\hat{\mu}^X}\|\cdot\|^2 = \frac{1}{Z}\int \|x\|^2 \exp\left(-\frac{\delta \hat{\mathcal{M}}}{\delta \rho}(\mu^X, x) - \frac{\lambda'}{2}\|x\|^2\right)\mathrm{d}x := \frac{Z'}{Z} \tag{53}$$

Now we bound Z' and Z respectively.

$$Z' \le \int \|x\|^2 \exp\left(\sqrt{2} - \frac{\lambda'}{2}\|x\|^2\right)\mathrm{d}x \lesssim \frac{\exp(\sqrt{2})d}{\lambda'},$$

$$Z \ge \int \exp\left(-\sqrt{3} - \frac{\lambda'}{2}\|x\|^2\right)\mathrm{d}x = \exp(-\sqrt{3})\left(\frac{2\pi}{\lambda'}\right)^{d/2}$$

Thus in order to ensure $\mathbb{E}_{\hat{\mu}^X}\|\cdot\|^2 = \frac{Z'}{Z} \lesssim \frac{\exp(\sqrt{2}+\sqrt{3})\lambda'^{\frac{d-2}{2}}}{(2\pi)^{\frac{d}{2}}}d \le d$, it suffices to choose $\lambda' \le 3\pi/25$.

KSD minimization Assume the score function s_{ρ_*} satisfies (22) and choose the kernel k to be (46), and the Stein kernel u_{ρ_*} satisfies $\sup_{x,x'\in\mathbb{R}^d}\max\{|u_{\rho_*}|,\|\nabla_x u_{\rho_*}\|,\|\nabla_x^2 u_{\rho_*}\|_{\mathsf{op}}\}\leq \mathscr{L}$ (Suzuki et al., 2023). We now prove the following objective

$$F(\rho) = \mathsf{KSD}(\rho) + \frac{\lambda'}{2}\mathbb{E}_{x\sim\rho}\|x\|^2 \tag{54}$$

satisfies Assumption 2.5, with KSD defined by $\mathsf{KSD}(\rho) = \iint u_{\rho_*}(x,x')\mathrm{d}\rho(x)\mathrm{d}\rho(x')$. The functional derivative of KSD is

$$\frac{\delta\mathsf{KSD}}{\delta\rho}(\rho,x) = \int u_{\rho_*}(x,x')\mathrm{d}\rho(x').$$

The functional derivative is bounded as

$$\left|\frac{\delta\mathsf{KSD}}{\delta\rho}(\rho,x)\right| \leq \int |u_{\rho_*}(x,x')|\mathrm{d}\rho(x') \leq \mathscr{L}.$$

Let $\hat{\mu}^X(x) = \exp\left(-\frac{\delta F}{\delta\rho}(\mu^X,x)\right)/Z$ where $Z = \int\exp\left(-\frac{\delta F}{\delta\rho}(\mu^X,x)\right)\mathrm{d}x$, and we have

$$\mathbb{E}_{\hat{\mu}^X}\|\cdot\|^2 = \frac{1}{Z}\int\|x\|^2\exp\left(-\frac{\delta\mathsf{KSD}}{\delta\rho}(\mu^X,x) - \frac{\lambda'}{2}\|x\|^2\right)\mathrm{d}x := \frac{Z'}{Z} \tag{55}$$

Now we bound Z' and Z respectively.

$$Z' \leq \int\|x\|^2\exp\left(\mathscr{L} - \frac{\lambda'}{2}\|x\|^2\right)\mathrm{d}x \lesssim \frac{\exp(\mathscr{L})d}{\lambda'},$$

$$Z \geq \int\exp\left(-\mathscr{L} - \frac{\lambda'}{2}\|x\|^2\right)\mathrm{d}x = \exp(-\mathscr{L})\left(\frac{2\pi}{\lambda'}\right)^{d/2}$$

Thus we have $\mathbb{E}_{\hat{\mu}^X}\|\cdot\|^2 = \frac{Z'}{Z} \lesssim \frac{\exp(2\mathscr{L})d\lambda'^{\frac{d}{2}-1}}{(2\pi)^{\frac{d}{2}}} \leq d$ for $\lambda' \leq (2\pi)^3\exp(-4\mathscr{L})$.

C.3 Verification of Assumption 2.6

Training mean-field neural networks Reformulate the objective (19) with $\mu_0 = \mathcal{N}(0,I_d)$:

$$F(\rho) = \frac{1}{n}\sum_{i=1}^n\ell(h(\rho;a_i),b_i) + \frac{\lambda'}{2}\mathbb{E}_{x\sim\rho}[\|x\|^2].$$

- If l is $\sqrt{\mathscr{L}}$-Lipschitz, we have $|\ell(h(\rho;a),b)| \leq \sqrt{\mathscr{L}}|h(\rho;a) - b|$. If $|h(x;a)| \leq \sqrt{\mathscr{L}}$, we have $|h(\rho;a)| \leq \sqrt{\mathscr{L}}$. Since $\mu_0 = \mathcal{N}(0,I_{2d})$, $\mathbb{E}_{x\sim\mu_0^X}[\|x\|^2] \lesssim d$. With $\lambda' \leq \min\{\mathscr{L},d\}$, we have $F(\mu_0^X) \lesssim \sqrt{\mathscr{L}}(\sqrt{\mathscr{L}} + \max_{i=1}^n|b_i|) + d$. We can normalize the data samples to ensure $\max_{i=1}^n|b_i| \lesssim d \wedge \sqrt{\mathscr{L}}$. Thus $F(\mu_0^X) \lesssim \mathscr{L} + d$.

- If $|h(x;a)| \leq \sqrt{\mathscr{L}}(1 + \|x\|)$, we have $|h(\mu_0^X;a)| \leq \sqrt{\mathscr{L}}\int(1 + \|x\|)\mu_0^X(\mathrm{d}x) \lesssim \sqrt{\mathscr{L}}d^{1/2}$. If ℓ is $\sqrt{\mathscr{L}}$-Lipschitz, we have $|l(h(\mu_0^X;a_i),b_i)| \leq \sqrt{\mathscr{L}}|h(\mu_0^X;a_i) - b_i| \lesssim \mathscr{L}d^{1/2} + \sqrt{\mathscr{L}}\max_{i=1}^n|b_i|$. We can normalize the data samples to ensure $\max_{i=1}^n|b_i| \lesssim d \wedge \sqrt{\mathscr{L}}$. Thus we have $F(\mu_0^X) \lesssim \mathscr{L}d + d$.

MMD minimization Reformulate the objective (20) with Gaussian RBF kernel ($\sigma' = \sigma$) and $\mu_0 = \mathcal{N}(0, I_d)$:

$$F(\rho) = \hat{\mathcal{M}}(\rho) + \frac{\lambda'}{2}\mathbb{E}_{x\sim\rho}\|x\|^2, \tag{56}$$

where

$$\hat{\mathcal{M}}(\rho) = \iiint p(x; z)p(x'; z')k(z, z')\mathrm{d}z\mathrm{d}z'\mathrm{d}(\rho \times \rho)(x, x') - 2\int \left(\frac{1}{n}\sum_{i=1}^n \int p(x; z)k(z, z_i)\mathrm{d}z\right)\mathrm{d}\rho(x)$$

$$= \frac{1}{3^{d/2}}\int \exp\left(-\frac{\|x - x'\|^2}{6\sigma^2}\right)\mathrm{d}(\rho \times \rho)(x, x') - \frac{2}{2^{d/2}}\frac{1}{n}\sum_{i=1}^n \int \exp\left(-\frac{\|x - z_i\|^2}{4\sigma^2}\right)\mathrm{d}\rho(x)$$

$$\leq \frac{1}{3^{d/2}}\int \exp\left(-\frac{\|x - x'\|^2}{6\sigma^2}\right)\mathrm{d}(\rho \times \rho)(x, x') \leq \frac{1}{3^{d/2}} \leq \mathscr{L}$$

Thus $F(\mu_0^X) = \hat{\mathcal{M}}(\mu_0^X) + \frac{\lambda'}{2}\mathbb{E}_{x\sim\mu_0^X}\|x\|^2 \lesssim \mathscr{L} + d$, which satisfies Assumption 2.6.

KSD minimization Consider the same objective in (21) with $\mu_0 = \mathcal{N}(0, I_d)$:

$$F(\rho) = \mathsf{KSD}(\rho) + \frac{\lambda'}{2}\mathbb{E}_{x\sim\rho}\|x\|^2.$$

If we choose kernel $k(x, x') = \exp\left(-\frac{\|x\|^2}{2\sigma_1^2} - \frac{\|x'\|^2}{2\sigma_1^2} - \frac{\|x-x'\|^2}{2\sigma_2^2}\right)$ and assume the score function of ρ_* satisfies $\max\{\|\nabla \log \rho_*(x)\|, \|\nabla^{\otimes 2}\log \rho_*(x)\|_{\mathsf{op}}, \|\nabla^{\otimes 3}\log\rho_*(x)\|_{\mathsf{op}}\} \leq \mathscr{L}(1 + \|x\|)$, then the Stein kernel u_{ρ_*} satisfies $\sup_{x,x'\in\mathbb{R}^d}\max\{|u_{\rho_*}|, \|\nabla_x u_{\rho_*}\|, \|\nabla_x^2 u_{\rho_*}\|_{\mathsf{op}}\} \leq \mathscr{L}$ according to the statement of Appendix A in Suzuki et al. (2023). We have

$$F(\mu_0^X) = \mathsf{KSD}(\mu_0^X) + \frac{\lambda'}{2}\mathbb{E}_{x\sim\mu_0^X}\|x\|^2$$

$$= \iint u_{\rho_*}(x, x')\mathrm{d}\mu^X(x)\mathrm{d}\mu^X(x') + \frac{\lambda'}{2}\mathbb{E}_{x\sim\mu_0^X}\|x\|^2$$

$$\lesssim \mathscr{L} + d,$$

which satisfies Assumption 2.6.

C.4   Verification of Assumption 2.7

Training mean-field neural networks Similar to examples of training mean-field neural networks above, we initialize $\mu_0^N = \mathcal{N}(0, I_{2Nd})$.

$$\mathbb{E}_{\mathbf{x}\sim\mu^N}F(\mu_{\mathbf{x}}) := \mathbb{E}_{\mathbf{x}\sim\mu^N}\frac{1}{n}\sum_{i=1}^n\left[\ell\left(\frac{1}{N}\sum_{s=1}^N h(x^s; a_i), b_i\right)\right] + \frac{\lambda'}{2}\mathbb{E}_{\mathbf{x}\sim\mu^N}\frac{1}{N}\sum_{s=1}^N\left[\|x^s\|^2\right],$$

where $\mathbf{x} = (x^1, ..., x^N)$, $x^i \sim \mu^i$ for $i = 1, ..., N$ and $\mu^N = \otimes_{i=1}^N \mu^i = \mathrm{Law}(x^1, ..., x^N)$.

- If $|h(x; a)| \leq \sqrt{\mathscr{L}}$ and ℓ is $\sqrt{\mathscr{L}}$-Lipschitz, and $\mathbb{E}_{\mathbf{x}_0\sim\mu_0^N}\frac{1}{n}\sum_{i=1}^n\left[\ell\left(\frac{1}{N}\sum_{i=1}^N h(x_0^i; a_i), b_i\right)\right] \lesssim \sqrt{\mathscr{L}}(\sqrt{\mathscr{L}} + \max_{i=1}^n |b_i|)$ and thus $\mathbb{E}_{\mu_0^N}F(\mu_{\mathbf{x}_0}) \lesssim \mathscr{L} + \sqrt{\mathscr{L}}\max_{i=1}^n |b_i| + d$. We can normalize the data samples to ensure $\max_{i=1}^n |b_i| \lesssim d \wedge \sqrt{\mathscr{L}}$. Thus we have $\mathbb{E}_{\mu_0^N}F(\mu_{\mathbf{x}_0}) = O(\mathscr{L} + d)$.

- If $|h(x; a)| \leq \sqrt{\mathscr{L}}(1+\|x\|)$ and ℓ is $\sqrt{\mathscr{L}}$-Lipschitz, $\mathbb{E}_{\mathbf{x}_0 \sim \mu_0^N} \frac{1}{n} \sum_{i=1}^{n} \left[\ell \left(\frac{1}{N} \sum_{s=1}^{N} h(x_0^s; a_i), b_i \right) \right] \leq$ $\sqrt{\mathscr{L}} \left(\sqrt{\mathscr{L}} \frac{1}{N} \sum_{s=1}^{N} (1 + \mathbb{E}_{\mathbf{x}_0 \sim \mu_0^N} \|x_0^s\|) + \max_{i=1}^{n} |b_i| \right) \lesssim \mathscr{L} d^{1/2} + \sqrt{\mathscr{L}} \max_{i=1}^{n} |b_i|$. We can normalize the data samples to ensure $\max_{i=1}^{n} |b_i| \lesssim d \wedge \sqrt{\mathscr{L}}$. Thus we have $\mathbb{E}_{\mu_0^N} F(\mu_{\mathbf{x}_0}) = O(\mathscr{L} d + d)$

MMD minimization Now we verify Assumption 2.7 for the example of density estimation. We consider the N-particle approximation of the objective (56) with the initialization $\mu_0^N = \mathcal{N}(0, I_{Nd})$.

$$\mathbb{E}_{\mu^N} \hat{\mathcal{M}}(\mu_{\mathbf{x}, \mathbf{y}})$$

$$:= \mathbb{E}_{\mathbf{x}, \mathbf{y} \sim \mu^N} \left[\frac{1}{N^2} \sum_{s=1}^{N} \sum_{t=1}^{N} \iint p(x^s; z) p(y^t; z') k(z, z') \mathrm{d}z \mathrm{d}z' - \frac{2}{nN} \sum_{i=1}^{n} \sum_{s=1}^{N} \int p(x^s; z) k(z, z_i) \mathrm{d}z \right]$$

$$\leq \mathbb{E}_{\mathbf{x}, \mathbf{y} \sim \mu^N} \left[\frac{1}{N^2} \sum_{s=1}^{N} \sum_{t=1}^{N} \iint p(x^s; z) p(y^t; z') k(z, z') \mathrm{d}z \mathrm{d}z' \right]$$

$$= \left(\frac{1}{\sqrt{3}} \right)^d \mathbb{E}_{\mathbf{x}, \mathbf{y} \sim \mu^N} \left[\frac{1}{N^2} \sum_{s=1}^{N} \sum_{t=1}^{N} \exp \left(-\frac{\|x^s - y^t\|^2}{6\sigma^2} \right) \right] \leq \left(\frac{1}{\sqrt{3}} \right)^d \leq \mathscr{L}$$

where $\mathbf{x} = (x^1, ..., x^N)$ and $\mathbf{y} = (y^1, ..., y^N)$. Thus we can upper bound $\mathbb{E}_{\mathbf{x}_0, \mathbf{y}_0 \sim \mu_0^N} F(\mu_{\mathbf{x}_0, \mathbf{y}_0})$ as follows:

$$\mathbb{E}_{\mathbf{x}_0, \mathbf{y}_0 \sim \mu_0^N} F(\mu_{\mathbf{x}_0, \mathbf{y}_0}) = \mathbb{E}_{\mathbf{x}_0, \mathbf{y}_0 \sim \mu_0^N} \hat{\mathcal{M}}(\mu_{\mathbf{x}, \mathbf{y}}) + \frac{\lambda'}{2} \mathbb{E}_{\mathbf{x}_0 \sim \mu_0^N} \frac{1}{N} \sum_{s=1}^{N} \left[\|x_0^s\|^2 \right] \lesssim \mathscr{L} + d$$

which satisfies Assumption 2.7.

KSD minimization Similar to the verification of Assumption 2.6 above, we have the following relation for $\mu_0^N = \mathcal{N}(0, I_{Nd})$ under the same assumptions on the score function and kernel:

$$\mathbb{E}_{\mathbf{x}_0 \sim \mu_0} F(\mu_{\mathbf{x}_0}) = \mathsf{KSD}(\mu_{\mathbf{x}_0}) + \frac{\lambda'}{2} \mathbb{E}_{\mathbf{x}_0 \sim \mu_0^N} \frac{1}{N} \sum_{s=1}^{N} \left[\|x_0^s\|^2 \right]$$

$$= \mathbb{E}_{\mathbf{x}_0 \sim \mu_0} \frac{1}{N^2} \sum_{i=1}^{N} \sum_{j=1}^{N} u_{\mu_*}(x_0^i, x_0^j) + \frac{\lambda'}{2} \mathbb{E}_{\mathbf{x}_0 \sim \mu_0^N} \frac{1}{N} \sum_{s=1}^{N} \left[\|x_0^s\|^2 \right] \lesssim \mathscr{L} + d,$$

which satisfies Assumption 2.7.

D Continuous-time results

In this section, we give the explicit rate of Theorem 2.1 and Theorem 2.2 proposed by Chen et al. (2023) with a specific choice of parameters and then provide the detailed proof of Theorem 3.1 and Theorem 3.2 by reparameterizing γ.

D.1 Proof of Theorem 3.1

Our proof is directly adapted from Theorem 2.1 in Chen et al. (2023) using hypocoercivity in Villani (2009). Chen et al. (2023) prove the Lyapunov functional

$$\mathcal{E}(\mu_t) = \mathcal{F}(\mu_t) + \mathsf{FI}_S(\mu_t \| \hat{\mu}_t) \tag{57}$$

is decaying along the MULD with $S = \begin{pmatrix} c & b \\ b & a \end{pmatrix} \otimes I_d$ and $\gamma = 1$. Let $A_t = \nabla_v$, $B_t = v \cdot \nabla_x - D_\rho F(\mu_t^X, x) \cdot \nabla_v$, $C_t = [A_t, B_t] = A_t B_t - B_t A_t = \nabla_x$ and $Y_t = (\|A_t u_t\|, \|A_t^2 u_t\|, \|C_t u_t\|, \|C_t A_t u_t\|)^\mathsf{T}$ where $u_t = \log \frac{\mu_t}{\hat{\mu}_t}$ and $\| \cdot \| := \| \cdot \|_{L^2(\mu_t)}$. More specifically, Chen et al. (2023) prove that

$$\frac{\mathrm{d}}{\mathrm{d}t} \mathcal{E}(\mu_t) \leq -Y_t^\mathsf{T} \mathcal{K} Y_t, \tag{58}$$

where

$$\mathcal{K} = \begin{pmatrix} 1 + 2a - 4\mathscr{L}b & -2b & -2a - 2\mathscr{L}c & 0 \\ 0 & 2a & -2\mathscr{L}c & -4b \\ 0 & 0 & 2b & 0 \\ 0 & 0 & 0 & 2c \end{pmatrix}.$$

The choice of a, b, c should satisfies $ac > b^2$ and $K \succ 0$. If we choose $a = c = 2\mathscr{L}$ and $b = 1$, the smallest eigenvalue of $\mathcal{K}$ is $\lambda_{\min}(\mathcal{K}) = 1$, and thus we have

$$\begin{aligned}
\frac{\mathrm{d}}{\mathrm{d}t}(\mathcal{E}(\mu_t) - \mathcal{E}(\mu_*)) &\leq -(\|A_t u_t\|^2 + \|A_t^2 u_t\|^2 + \|C_t u_t\|^2 + \|C_t A_t u_t\|^2) \\
&\leq -(\|A_t u_t\|^2 + \|C_t u_t\|^2) = -\frac{1}{2}\mathsf{FI}(\mu_t\|\hat{\mu}_t) - \frac{1}{2}\mathsf{FI}(\mu_t\|\hat{\mu}_t) \\
&\leq -\mathscr{C}_{\mathsf{LSI}}\mathsf{KL}(\mu_t\|\hat{\mu}_t) - \frac{1}{2\lambda_{\max}(S)}\mathsf{FI}_S(\mu_t\|\hat{\mu}_t) \\
&\leq -\mathscr{C}_{\mathsf{LSI}}(\mathcal{F}(\mu_t) - \mathcal{F}(\mu_*)) - \frac{1}{4\mathscr{L}+2}\mathsf{FI}_S(\mu_t\|\hat{\mu}_t) \\
&\leq -\frac{\mathscr{C}_{\mathsf{LSI}}}{6\mathscr{L}}(\mathcal{E}(\mu_t) - \mathcal{E}(\mu_*))
\end{aligned}$$

Applying Grönwall's inequality, we obtain

$$\mathcal{F}(\mu_t) - \mathcal{F}(\mu_*) \leq \mathcal{E}(\mu_t) - \mathcal{E}(\mu_*) \leq (\mathcal{E}(\mu_0) - \mathcal{E}(\mu_*)) \exp\left(-\frac{\mathscr{C}_{\mathsf{LSI}}}{6\mathscr{L}}t\right). \tag{59}$$

Note that the proof in Chen et al. (2023) also considers the approximation technique to remove some restrictive assumptions they make, which we omit in our proof. Now we consider a more general γ in the proof above. Analogous to the proof of Lemma 32 in Villani (2009), if we incorporate a general γ, the diagonal elements of upper triangular matrix $\mathcal{K}$ will become $(\gamma + 2\gamma a - 4\mathscr{L}b, 2\gamma a, 2b, 2\gamma c)$. If we choose $\gamma = \sqrt{\mathscr{L}}$, $b = 1/\sqrt{\mathscr{L}}$, $a = 2$ and $c = 1/\mathscr{L}$, the smallest eigenvalue of K will become $\lambda_{\min}(\mathcal{K}) = 2/\sqrt{\mathscr{L}}$. Similar to the previous proof, we have

$$\begin{aligned}
\frac{\mathrm{d}}{\mathrm{d}t}(\mathcal{E}(\mu_t) - \mathcal{E}(\mu_*)) &\leq -\frac{2}{\sqrt{\mathscr{L}}}(\|A_t u_t\|^2 + \|A_t^2 u_t\|^2 + \|C_t u_t\|^2 + \|C_t A_t u_t\|^2) \\
&\leq -\frac{2}{\sqrt{\mathscr{L}}}(\|A_t u_t\|^2 + \|C_t u_t\|^2) = -\frac{1}{\sqrt{\mathscr{L}}}\mathsf{FI}(\mu_t\|\hat{\mu}_t) - \frac{1}{\sqrt{\mathscr{L}}}\mathsf{FI}(\mu_t\|\hat{\mu}_t) \\
&\leq -\frac{2\mathscr{C}_{\mathsf{LSI}}}{\sqrt{\mathscr{L}}}\mathsf{KL}(\mu_t\|\hat{\mu}_t) - \frac{1}{\lambda_{\max}(S)\sqrt{\mathscr{L}}}\mathsf{FI}_S(\mu_t\|\hat{\mu}_t) \\
&\leq -\frac{2\mathscr{C}_{\mathsf{LSI}}}{\sqrt{\mathscr{L}}}(\mathcal{F}(\mu_t) - \mathcal{F}(\mu_*)) - \frac{1}{3\sqrt{\mathscr{L}}}\mathsf{FI}_S(\mu_t\|\hat{\mu}_t) \\
&\leq -\frac{\mathscr{C}_{\mathsf{LSI}}}{3\sqrt{\mathscr{L}}}(\mathcal{E}(\mu_t) - \mathcal{E}(\mu_*))
\end{aligned}$$

where the fourth inequality follows from $\lambda_{\max}(S) = \frac{\frac{1}{\mathscr{L}} + 2 + \sqrt{\frac{1}{\mathscr{L}^2} + 4}}{2} \leq \frac{1}{\mathscr{L}} + 2 \leq 3$. Applying Grönwall's inequality, we obtain

$$\mathcal{F}(\mu_t) - \mathcal{F}(\mu_*) \leq \mathcal{E}(\mu_t) - \mathcal{E}(\mu_*) \leq (\mathcal{E}(\mu_0) - \mathcal{E}(\mu_*)) \exp\left(-\frac{\mathscr{C}_{\mathsf{LSI}}}{3\sqrt{\mathscr{L}}}t\right), \tag{60}$$

which completes the proof of Theorem 3.1. Eq. (60) exhibits a faster rate than the rate of Eq. (59).

D.2   Proof of Theorem 3.2

Our proof is directly adapted from Theorem 2.2 in Chen et al. (2023) using hypocoercivity in Villani (2009). Chen et al. (2023) prove that the Lyapunov functional

$$\mathcal{E}^N(\mu_t^N) = \mathcal{F}^N(\mu_t^N) + \mathsf{FI}_S^N(\mu_t^N \| \mu_*^N) \tag{61}$$

is decaying along the N-ULD with $S = \begin{pmatrix} c & b \\ b & a \end{pmatrix} \otimes I_d$ and $\gamma = 1$. Let $u_t^N = \log \frac{\mu_t^N}{\mu_*^N}$, $\|\cdot\| := \|\cdot\|_{L^2(\mu_t^N)}$ and

$$Y_t^N = (\|\nabla_{\mathbf{v}} u_t^N\|, \|\nabla_{\mathbf{v}}^2 u_t^N\|, \|\nabla_{\mathbf{x}} u_t^N\|, \|\nabla_{\mathbf{x}} \nabla_{\mathbf{v}} u_t^N\|)^{\mathsf{T}}.$$

Chen et al. (2023) prove that

$$\frac{\mathrm{d}}{\mathrm{d}t} \mathcal{E}^N(\mu_t^N) \leq -(Y_t^N)^{\mathsf{T}} \mathcal{K} Y_t^N \tag{62}$$

where

$$\mathcal{K} = \begin{pmatrix} 1 + 2a - 4\mathscr{L}b & -2b & -2a & 0 \\ 0 & 2a & -4\mathscr{L}c & -4b \\ 0 & 0 & 2b & 0 \\ 0 & 0 & 0 & 2c \end{pmatrix}.$$

The choice of a, b, c should satisfies $ac > b^2$ and $K \succ 0$. If we choose $a = c = 2\mathscr{L}$ and $b = 1$, the smallest eigenvalue of K is $\lambda_{\min}(\mathcal{K}) = 1$, and thus we have

$$\begin{aligned} \frac{\mathrm{d}}{\mathrm{d}t} \mathcal{E}^N(\mu_t^N) &\leq -(\|\nabla_{\mathbf{v}} u_t^N\|^2 + \|\nabla_{\mathbf{v}}^2 u_t^N\|^2 + \|\nabla_{\mathbf{x}} u_t^N\|^2 + \|\nabla_{\mathbf{x}} \nabla_{\mathbf{v}} u_t^N\|^2) \\ &\leq -(\|\nabla_{\mathbf{v}} u_t^N\|^2 + \|\nabla_{\mathbf{x}} u_t^N\|^2) = -\mathsf{FI}(\mu_t^N \| \mu_*^N) \end{aligned} \tag{63}$$

Since μ_*^N does not satisfy the uniform LSI, we can not utilize the same technique to upper bound $-\mathsf{FI}(\mu_t^N \| \mu_*^N)$. Chen et al. (2022) and Chen et al. (2023) obtain the lower bound of the relative Fisher information $\mathsf{FI}(\mu_t^N \| \mu_*^N)$ using other technique to circumvent the uniform LSI of μ_*^N. We will directly provide the conclusion instead of providing many details about that technique in this paper, and we refer our readers to Chen et al. (2022, 2023) for the precise proof. Chen et al. (2023) propose that

$$\begin{aligned} \mathsf{FI}(\mu_t^N \| \mu_*^N) &= \frac{1}{2}\mathsf{FI}(\mu_t^N \| \mu_*^N) + \frac{1}{2}\mathsf{FI}(\mu_t^N \| \mu_*^N) \\ &\geq \frac{1}{2}\left[2(1-\varepsilon)\mathscr{C}_{\mathsf{LSI}} - \frac{\mathscr{L}}{N}\left(16 + 12(\varepsilon^{-1} - 1)\frac{\mathscr{L}}{\mathscr{C}_{\mathsf{LSI}}}\right)\right](\mathcal{F}^N(\mu_t^N) - N\mathcal{F}(\mu_*)) \\ &\quad + \frac{1}{2}\mathsf{FI}(\mu_t^N \| \mu_*^N) - \frac{\mathscr{L}d}{\mathscr{C}_{\mathsf{LSI}}}(5\mathscr{C}_{\mathsf{LSI}} + 3(\varepsilon^{-1} - 1)\mathscr{L}) \end{aligned}$$

for $\varepsilon \in (0, 1)$. If we choose $\varepsilon = 1/2$ and $N \geq \frac{32\mathscr{L}}{\mathscr{C}_{\mathsf{LSI}}} + \frac{24\mathscr{L}^2}{\mathscr{C}_{\mathsf{LSI}}^2}$, we have

$$
\begin{aligned}
\mathsf{FI}(\mu_t^N \| \mu_*^N) &\geq \frac{\mathscr{C}_{\mathsf{LSI}}}{4}(\mathcal{F}^N(\mu_t^N) - N\mathcal{F}(\mu_*)) + \frac{1}{2\lambda_{\mathsf{max}}(S)}\mathsf{FI}_S(\mu_t^N \| \mu_*^N) - \frac{\mathscr{L}d}{\mathscr{C}_{\mathsf{LSI}}}(5\mathscr{C}_{\mathsf{LSI}} + 3\mathscr{L}) \\
&\geq \frac{\mathscr{C}_{\mathsf{LSI}}}{4}(\mathcal{F}^N(\mu_t^N) - N\mathcal{F}(\mu_*)) + \frac{1}{6\mathscr{L}}\mathsf{FI}_S(\mu_t^N \| \mu_*^N) - \frac{\mathscr{L}d}{\mathscr{C}_{\mathsf{LSI}}}(5\mathscr{C}_{\mathsf{LSI}} + 3\mathscr{L}) \\
&\geq \frac{\mathscr{C}_{\mathsf{LSI}}}{24\mathscr{L}}(\mathcal{E}^N(\mu_t^N) - N\mathcal{E}(\mu_*)) - \frac{\mathscr{L}d}{\mathscr{C}_{\mathsf{LSI}}}(5\mathscr{C}_{\mathsf{LSI}} + 3\mathscr{L})
\end{aligned}
$$

Combining (63) with the lower bound of Fisher information above, we obtain

$$
\frac{\mathrm{d}}{\mathrm{d}t}(\mathcal{E}^N(\mu_t^N) - N\mathcal{E}(\mu_*)) \leq -\frac{\mathscr{C}_{\mathsf{LSI}}}{24\mathscr{L}}(\mathcal{E}^N(\mu_t^N) - N\mathcal{E}(\mu_*)) + \frac{\mathscr{L}d}{\mathscr{C}_{\mathsf{LSI}}}(5\mathscr{C}_{\mathsf{LSI}} + 3\mathscr{L})
$$

Applying Grönwall's inequality, we obtain

$$
\begin{aligned}
\mathcal{F}^N(\mu_t^N) - N\mathcal{F}(\mu_*) &\leq \mathcal{E}^N(\mu_t^N) - N\mathcal{E}(\mu_*) \\
&\leq (\mathcal{E}^N(\mu_0^N) - N\mathcal{E}(\mu_*)) \exp\left(-\frac{\mathscr{C}_{\mathsf{LSI}}}{24\mathscr{L}}t\right) + \frac{\mathscr{L}dt}{\mathscr{C}_{\mathsf{LSI}}}(5\mathscr{C}_{\mathsf{LSI}} + 3\mathscr{L})\exp\left(-\frac{\mathscr{C}_{\mathsf{LSI}}}{24\mathscr{L}}t\right) \\
&\leq (\mathcal{E}^N(\mu_0^N) - N\mathcal{E}(\mu_*)) \exp\left(-\frac{\mathscr{C}_{\mathsf{LSI}}}{24\mathscr{L}}t\right) + \frac{120\mathscr{L}^2 d}{\mathscr{C}_{\mathsf{LSI}}} + \frac{72\mathscr{L}^3 d}{\mathscr{C}_{\mathsf{LSI}}^2}
\end{aligned}
$$

(64)

where the last inequality follows from $\exp(-x) \leq (1 + x)^{-1}$ for $x > -1$. Now we consider a more general γ in the proof above. Analogous to the proof of Lemma 32 in Villani (2009), if we incorporate γ, the diagonal elements of upper triangular matrix $\mathcal{K}$ will become $(\gamma + 2\gamma a - 4\mathscr{L}b, 2\gamma a, 2b, 2\gamma c)$. If we choose $\gamma = \sqrt{\mathscr{L}}$, $b = 1/\sqrt{\mathscr{L}}$, $a = 2$ and $c = 1/\mathscr{L}$, the smallest eigenvalue of K will become $\lambda_{\mathsf{min}}(\mathscr{K}) = 2/\sqrt{\mathscr{L}}$. Similar to the previous proof, we have

$$
\begin{aligned}
\frac{\mathrm{d}}{\mathrm{d}t}(\mathcal{E}^N(\mu_t^N) - N\mathcal{E}(\mu_*)) &\leq -\frac{2}{\sqrt{\mathscr{L}}}(\|\nabla_{\mathbf{v}} u_t^N\|^2 + \|\nabla_{\mathbf{v}}^2 u_t^N\|^2 + \|\nabla_{\mathbf{x}} u_t^N\|^2 + \|\nabla_{\mathbf{x}}\nabla_{\mathbf{v}} u_t^N\|^2) \\
&\leq -\frac{2}{\sqrt{\mathscr{L}}}(\|\nabla_{\mathbf{v}} u_t^N\|^2 + \|\nabla_{\mathbf{x}} u_t^N\|^2) = -\frac{2}{\sqrt{\mathscr{L}}}\mathsf{FI}(\mu_t^N \| \mu_*^N) \\
&\leq -\frac{\mathscr{C}_{\mathsf{LSI}}}{2\sqrt{\mathscr{L}}}(\mathcal{F}^N(\mu_t^N) - N\mathcal{F}(\mu_*)) - \frac{1}{\lambda_{\mathsf{max}}(S)\sqrt{\mathscr{L}}}\mathsf{FI}_S(\mu_t^N \| \mu_*^N) \\
&\quad + \frac{2\sqrt{\mathscr{L}}d}{\mathscr{C}_{\mathsf{LSI}}}(5\mathscr{C}_{\mathsf{LSI}} + 3\mathscr{L}) \\
&\leq -\frac{\mathscr{C}_{\mathsf{LSI}}}{2\sqrt{\mathscr{L}}}(\mathcal{F}^N(\mu_t^N) - N\mathcal{F}(\mu_*)) - \frac{1}{3\sqrt{\mathscr{L}}}\mathsf{FI}_S(\mu_t^N \| \mu_*^N) + \frac{2\sqrt{\mathscr{L}}d}{\mathscr{C}_{\mathsf{LSI}}}(5\mathscr{C}_{\mathsf{LSI}} + 3\mathscr{L}) \\
&\leq -\frac{\mathscr{C}_{\mathsf{LSI}}}{6\sqrt{\mathscr{L}}}(\mathcal{E}^N(\mu_t^N) - N\mathcal{E}(\mu_*)) + \frac{2\sqrt{\mathscr{L}}d}{\mathscr{C}_{\mathsf{LSI}}}(5\mathscr{C}_{\mathsf{LSI}} + 3\mathscr{L})
\end{aligned}
$$

Applying Grönwall's inequality, we obtain

$$
\mathcal{F}^N(\mu_t^N) - N\mathcal{F}(\mu_*) \leq \mathcal{E}^N(\mu_t^N) - N\mathcal{E}(\mu_*) \leq \mathcal{E}_0^N \exp\left(-\frac{\mathscr{C}_{\mathsf{LSI}}}{6\sqrt{\mathscr{L}}}t\right) + \frac{60\mathscr{L}d}{\mathscr{C}_{\mathsf{LSI}}} + \frac{36\mathscr{L}^2 d}{\mathscr{C}_{\mathsf{LSI}}^2} \tag{65}
$$

where $\mathcal{E}_0^N := \mathcal{E}^N(\mu_0^N) - N\mathcal{E}(\mu_*)$. This completes the proof of Theorem 3.2. The convergence rate exhibited in Eq. (65) is faster and incurs a smaller bias than the rate exhibited in Eq. (64).

E Discretization analysis

In this section, we provide the proof of Theorem 3.3 and Theorem 3.4 establishing the global convergence of the discrete-time-space processes. Our discretization analysis is unified for the MULA and NULA.

E.1 Proof of Theorem 3.3

Suppose $\mathbf{Q}_{Nh}$ is the joint law of the MULD for $t \in [0, Nh]$ and $\mathbf{P}_{Nh}$ is the joint law of the MULA for $t \in [kh, (k+1)h]$ and $k = 0, 1, ..., K-1$. Applying Girsanov's theorem (Lemma 10), we have

$$
\mathsf{KL}(\mathbf{Q}_{Kh} \| \mathbf{P}_{Kh}) = \mathbb{E}_{\mathbf{Q}_{Kh}} \log \frac{\mathrm{d}\mathbf{Q}_{Kh}}{\mathrm{d}\mathbf{P}_{Kh}}
$$

$$
= \mathbb{E}_{\mathbf{Q}_{Kh}} \sum_{k=0}^{K-1} \left(-\frac{1}{\sqrt{2\gamma}} \int_{kh}^{(k+1)h} \left\langle \begin{pmatrix} 0 \\ D_\rho F(\mu_t^X, x_t) - D_\rho F(\mu_{kh}^X, x_{kh}) \end{pmatrix}, \mathrm{dB}_t \right\rangle \right.
$$

$$
\left. + \frac{1}{4\gamma} \int_{kh}^{(k+1)h} \left\| D_\rho F(\mu_t^X, x_t) - D_\rho F(\mu_{kh}^X, x_{kh}) \right\|^2 \mathrm{d}t \right)
$$

$$
= \frac{1}{4\gamma} \sum_{k=0}^{K-1} \int_{kh}^{(k+1)h} \mathbb{E}_{\mathbf{Q}_{Kh}} \left\| D_\mu F(\mu_t^X, x_t) - D_\mu F(\mu_{kh}^X, x_{kh}) \right\|^2 \mathrm{d}t
$$

And we obtain

$$
\mathsf{KL}(\mathbf{Q}_{Kh} \| \mathbf{P}_{Kh}) = \frac{1}{4\gamma} \sum_{k=0}^{K-1} \int_{kh}^{(k+1)h} \mathbb{E}_{\mathbf{Q}_{Kh}} \left\| D_\rho F(\mu_t^X, x_t) - D_\rho F(\mu_{kh}^X, x_{kh}) \right\|^2 \mathrm{d}t
$$

$$
\leq \frac{\mathscr{L}^2}{2\gamma} \sum_{k=0}^{K-1} \int_{kh}^{(k+1)h} \mathbb{E}_{\mathbf{Q}_{Kh}} \|x_t - x_{kh}\|^2 + W_1^2(\mu_t^X, \mu_{kh}^X) \mathrm{d}t
$$

$$
\leq \frac{\mathscr{L}^2}{2\gamma} \sum_{k=0}^{K-1} \int_{kh}^{(k+1)h} \mathbb{E}_{\mathbf{Q}_{Kh}} \|x_t - x_{kh}\|^2 + \mathbb{E}_{\mathbf{Q}_{Kh}} \|x_t - x_{kh}\|^2 \mathrm{d}t
$$

$$
= \frac{\mathscr{L}^2}{\gamma} \sum_{k=0}^{K-1} \int_{kh}^{(k+1)h} \mathbb{E}_{\mathbf{Q}_{Kh}} \|x_t - x_{kh}\|^2 \mathrm{d}t
$$

where the first inequality follows from Assumption 2.2 and the last inequality follows from Lemma 7 and the inequality $\left(\frac{1}{n} \sum_{i=1}^{n} x_i \right)^2 \leq \frac{1}{n} \sum_{i=1}^{n} x_i^2$:

$$
\mathbb{E}_{\mathbf{Q}_{Kh}} \|x_t - x_{kh}\|^2 \leq 16\mathscr{L}^2 h^4 \mathbb{E}_{\mathbf{Q}_{Kh}} \|x_{kh}\|^2 + 64h^2 \mathbb{E}_{\mathbf{Q}_{Kh}} \|v_{kh}\|^2 + 16\mathscr{L}^2 h^4 + 32\gamma h^3 d
$$

Combined with Lemma 8 and $\gamma = \sqrt{\mathscr{L}}$, the discretization error is upper bounded as follows:

$$
\mathsf{KL}(\mathbf{Q}_{Kh} \| \mathbf{p}_{Kh}) \leq \frac{16\mathscr{L}^4 h^5 K}{\gamma} \max_{0 \leq k \leq K} \mathbb{E}_{\mathbf{Q}_{Kh}} \|x_{kh}\|^2 + \frac{64\mathscr{L}^2 h^3 K}{\gamma} \max_{0 \leq k \leq K} \mathbb{E}_{\mathbf{Q}_{Kh}} \|v_{kh}\|^2
$$

$$
+ \frac{16\mathscr{L}^4 h^5 K}{\gamma} + 32\mathscr{L}^2 h^4 K d
$$

$$
\lesssim \frac{\mathscr{L}^{9/2} h^5 K d}{\mathscr{C}_{\mathsf{LSI}}} + \frac{\mathscr{L}^{5/2} h^3 K d}{\mathscr{C}_{\mathsf{LSI}}} + \mathscr{L}^{7/2} h^5 K + \mathscr{L}^2 h^4 K d
$$

$$
= \frac{\mathscr{L}^{9/2} h^4 T d}{\mathscr{C}_{\mathsf{LSI}}} + \frac{\mathscr{L}^{5/2} h^2 T d}{\mathscr{C}_{\mathsf{LSI}}} + \mathscr{L}^{7/2} h^4 T + \mathscr{L}^2 h^3 T d
$$

where $T = Kh$. By Lemma 3 and Theorem 3.1, we obtain

$$\mathsf{KL}(\mu_t\|\mu_*) \leq \mathcal{F}(\mu_t) - \mathcal{F}(\mu_*) \leq (\mathcal{E}(\mu_0) - \mathcal{E}(\mu_*)) \exp\left(-\frac{\mathscr{C}_{\mathsf{LSI}}}{3\sqrt{\mathscr{L}}}t\right) \tag{66}$$

Combining with (66), we upper bound the TV distance between $\bar{\mu}_K$, the probability measure of MULA at Kh and μ_*, the limiting distribution of MULD as follows:

$$
\begin{aligned}
\|\bar{\mu}_K - \mu_*\|_{\mathsf{TV}} &\leq \|\bar{\mu}_K - \mu_{Kh}\|_{\mathsf{TV}} + \|\mu_{Kh} - \mu_*\|_{\mathsf{TV}} \\
&= \|\mu_{Kh} - \bar{\mu}_K\|_{\mathsf{TV}} + \|\mu_{Kh} - \mu_*\|_{\mathsf{TV}} \\
&\lesssim \sqrt{\mathsf{KL}(\mu_{Kh}\|\bar{\mu}_K)} + \sqrt{\mathsf{KL}(\mu_{Kh}\|\mu_*)} \\
&\lesssim \sqrt{\mathsf{KL}(\mathbf{Q}_{Kh}\|\mathbf{p}_{Kh})} + \sqrt{\mathsf{KL}(\mu_{Kh}\|\mu_*)} \\
&\lesssim \frac{\mathscr{L}^{9/4}h^2T^{1/2}d^{1/2}}{\mathscr{C}_{\mathsf{LSI}}^{1/2}} + \frac{\mathscr{L}^{5/4}hT^{1/2}d^{1/2}}{\mathscr{C}_{\mathsf{LSI}}^{1/2}} + \mathscr{L}^{7/4}h^2T^{1/2} + \mathscr{L}h^{3/2}T^{1/2}d^{1/2} \\
&\quad + (\mathcal{E}(\mu_0) - \mathcal{E}(\mu_*))^{1/2}\exp\left(-\mathscr{C}_{\mathsf{LSI}}T/6\sqrt{\mathscr{L}}\right)
\end{aligned}
$$

where the first inequality follows from the triangle inequality of TV distance; the second inequality follows from Pinsker's inequality, and the fourth inequality follows from the data processing inequality. In order to ensure $\|\mu_{Kh} - \mu_*\|_{\mathsf{TV}} \leq \frac{1}{2}\epsilon$, it suffices to choose $T = Kh = \widetilde{\Theta}\left(\frac{\sqrt{\mathscr{L}}}{\mathscr{C}_{\mathsf{LSI}}}\right)$. In order to ensure $\|\bar{\mu}_K - \mu_{Kh}\|_{\mathsf{TV}} \leq \frac{1}{2}\epsilon$, it suffices to choose the stepsize

$$h = \Theta\left(\frac{\mathscr{C}_{\mathsf{LSI}}^{1/2}\epsilon}{\mathscr{L}^{5/4}T^{1/2}d^{1/2}}\right) = \widetilde{\Theta}\left(\frac{\mathscr{C}_{\mathsf{LSI}}\epsilon}{\mathscr{L}^{3/2}d^{1/2}}\right), \tag{67}$$

and the mixing time

$$K = \frac{T}{h} = \widetilde{\Theta}\left(\frac{\mathscr{L}^2 d^{1/2}}{\mathscr{C}_{\mathsf{LSI}}^2 \epsilon}\right). \tag{68}$$

The choice of T, h, K above ensures $\|\bar{\mu}_K - \mu_*\|_{\mathsf{TV}} \leq \epsilon$.

E.2 Proof of Theorem 3.4

Suppose Q_{Nh}^i is the joint law of the N-ULD for the i-th particle and $t \in [0, Kh]$; P_{Nh}^i is the joint law of the NULA for the i-th particle. Applying Girsanov's theorem (Lemma 10), we have

$$
\begin{aligned}
\frac{1}{N}\sum_{i=1}^{N}\mathsf{KL}(\mathbf{Q}_{Kh}^i\|\mathbf{P}_{Kh}^i) &= \frac{1}{4\gamma}\sum_{k=0}^{K-1}\int_{kh}^{(k+1)h}\frac{1}{N}\sum_{i=1}^{N}\mathbb{E}_{\mathbf{Q}_{Kh}^i}\left\|D_\rho F(\mu_{\mathbf{x}_t}, x_t^i) - D_\rho F(\mu_{\mathbf{x}_{kh}}, x_{kh}^i)\right\|^2 \mathrm{d}t \\
&\leq \frac{\mathscr{L}^2}{2\gamma}\sum_{k=0}^{K-1}\int_{kh}^{(k+1)h}\frac{1}{N}\sum_{i=1}^{N}\mathbb{E}_{\mathbf{Q}_{Kh}^i}\|x_t^i - x_{kh}^i\|^2 + W_1^2(\mu_{\mathbf{x}_t}, \mu_{\mathbf{x}_{kh}})\mathrm{d}t \\
&\leq \frac{\mathscr{L}^2}{\gamma}\sum_{k=0}^{K-1}\int_{kh}^{(k+1)h}\frac{1}{N}\sum_{i=1}^{N}\mathbb{E}_{\mathbf{Q}_{Kh}^i}\|x_t^i - x_{kh}^i\|^2\mathrm{d}t \\
&\leq \frac{16\mathscr{L}^4h^5}{\gamma}\frac{1}{N}\sum_{i=1}^{N}\sum_{k=1}^{K}\mathbb{E}_{\mathbf{Q}_{Kh}^i}\|x_{kh}^i\|^2 + \frac{64\mathscr{L}^2h^3}{\gamma}\frac{1}{N}\sum_{i=1}^{N}\sum_{k=1}^{K}\mathbb{E}_{\mathbf{Q}_{Kh}^i}\|v_{kh}\|^2 \\
&\quad + \frac{16\mathscr{L}^4h^5K}{\gamma} + 32\mathscr{L}^2h^4Kd
\end{aligned}
$$

where the first inequality follows from Assumption 2.2 and the last inequality follows from Lemma 7 and the inequality $\left(\frac{1}{n} \sum_{i=1}^{n} x_i \right)^2 \leq \frac{1}{n} \sum_{i=1}^{n} x_i^2$:

$$\mathbb{E}_{\mathbf{Q}_{Kh}^i} \|x_t^i - x_{kh}^i\|^2 \leq 16 \mathscr{L}^2 h^4 \mathbb{E}_{\mathbf{Q}_{Kh}^i} \|x_{kh}^i\|^2 + 64 h^2 \mathbb{E}_{\mathbf{Q}_{Kh}^i} \|v_{kh}^i\|^2 + 16 \mathscr{L}^2 h^4 + 32 \gamma h^3 d$$

for $t \in [kh, (k+1)h]$ and $k = 0, 1, ..., K-1$. Combining Lemma 9 and $\gamma = \sqrt{\mathscr{L}}$, the discretization error is upper bounded as follows:

$$\frac{1}{N} \sum_{i=1}^{N} \mathsf{KL}(\mathbf{Q}_{Kh}^i \| \mathbf{P}_{Kh}^i) \leq \frac{16 \mathscr{L}^4 h^5 K}{\gamma} \frac{1}{N} \sum_{i=1}^{N} \max_{0 \leq k \leq K} \mathbb{E}_{\mathbf{Q}_{Kh}^i} \|x_{kh}^i\|^2 + \frac{64 \mathscr{L}^2 h^3 K}{\gamma} \frac{1}{N} \sum_{i=1}^{N} \max_{0 \leq k \leq K} \mathbb{E}_{\mathbf{Q}_{Kh}^i} \|v_{kh}^i\|^2$$

$$+ \frac{16 \mathscr{L}^4 h^5 K}{\gamma} + 32 \mathscr{L}^2 h^4 K d$$

$$\lesssim \frac{\mathscr{L}^{9/2} h^5 K d}{\mathscr{C}_{\mathsf{LSI}}} + \frac{\mathscr{L}^{5/2} h^3 K d}{\mathscr{C}_{\mathsf{LSI}}} + \mathscr{L}^{7/2} h^5 K + \mathscr{L}^2 h^4 K d$$

$$= \frac{\mathscr{L}^{9/2} h^4 T d}{\mathscr{C}_{\mathsf{LSI}}} + \frac{\mathscr{L}^{5/2} h^2 T d}{\mathscr{C}_{\mathsf{LSI}}} + \mathscr{L}^{7/2} h^4 T + \mathscr{L}^2 h^3 T d$$

where $T = Kh$. By Lemma 4 and Theorem 3.2, we obtain

$$\frac{1}{N} \mathsf{KL}(\mu_T^N \| \mu_*^{\otimes N}) \leq \frac{1}{N} \mathcal{F}^N(\mu_T^N) - \mathcal{F}(\mu_*) \leq \frac{\mathcal{E}_0^N}{N} \exp\left(-\frac{\mathscr{C}_{\mathsf{LSI}}}{6\sqrt{\mathscr{L}}} T \right) + \frac{60 \mathscr{L} d}{N \mathscr{C}_{\mathsf{LSI}}} + \frac{36 \mathscr{L}^2 d}{N \mathscr{C}_{\mathsf{LSI}}^2}, \qquad (69)$$

where $\mathcal{E}_0^N := \mathcal{E}^N(\mu_0^N) - N \mathcal{E}(\mu_*)$. Combining with (69), we upper bound the averaged TV distance between $\bar{\mu}_K^i$ and μ_* over N particles as follows:

$$\frac{1}{N} \sum_{i=1}^{N} \|\bar{\mu}_K^i - \mu_*\|_{\mathsf{TV}} \leq \frac{1}{N} \sum_{i=1}^{N} \|\bar{\mu}_K^i - \mu_{Kh}^i\|_{\mathsf{TV}} + \frac{1}{N} \sum_{i=1}^{N} \|\mu_{Kh}^i - \mu_*\|_{\mathsf{TV}}$$

$$= \frac{1}{N} \sum_{i=1}^{N} \|\mu_{Kh}^i - \bar{\mu}_K^i\|_{\mathsf{TV}} + \frac{1}{N} \sum_{i=1}^{N} \|\mu_{Kh}^i - \mu_*\|_{\mathsf{TV}}$$

$$\lesssim \frac{1}{N} \sum_{i=1}^{N} \sqrt{\mathsf{KL}(\mu_{Kh}^i \| \bar{\mu}_K^i)} + \frac{1}{N} \sum_{i=1}^{N} \sqrt{\mathsf{KL}(\mu_{Kh}^i \| \mu_*)}$$

$$\lesssim \sqrt{\frac{1}{N} \sum_{i=1}^{N} \mathsf{KL}(\mu_{Kh}^i \| \bar{\mu}_K^i)} + \sqrt{\frac{1}{N} \sum_{i=1}^{N} \mathsf{KL}(\mu_{Kh}^i \| \mu_*)}$$

$$\leq \sqrt{\frac{1}{N} \sum_{i=1}^{N} \mathsf{KL}(\mathbf{Q}_{Kh}^i \| \mathbf{P}_{Kh}^i)} + \sqrt{\frac{1}{N} \mathsf{KL}(\mu_{Kh}^N \| \mu_*^{\otimes N})}$$

$$\leq \sqrt{\frac{1}{N} \sum_{i=1}^{N} \mathsf{KL}(\mathbf{Q}_{Kh}^i \| \mathbf{P}_{Kh}^i)} + \sqrt{\frac{1}{N} \mathcal{F}^N(\mu_{Kh}^N) - \mathcal{F}(\mu_*)}$$

$$\lesssim \frac{\mathscr{L}^{9/4} h^2 T^{1/2} d^{1/2}}{\mathscr{C}_{\mathsf{LSI}}^{1/2}} + \frac{\mathscr{L}^{5/4} h T^{1/2} d^{1/2}}{\mathscr{C}_{\mathsf{LSI}}^{1/2}} + \mathscr{L}^{7/4} h^2 T^{1/2} + \mathscr{L} h^{3/2} T^{1/2} d^{1/2}$$

$$+ \left(\frac{1}{N} \mathcal{E}^N(\mu_0^N) - \mathcal{E}(\mu_*) \right)^{1/2} \exp\left(-\mathscr{C}_{\mathsf{LSI}} T / 12 \sqrt{\mathscr{L}} \right) + \frac{\mathscr{L}^{1/2} d^{1/2}}{N^{1/2} \mathscr{C}_{\mathsf{LSI}}^{1/2}} + \frac{\mathscr{L} d^{1/2}}{N^{1/2} \mathscr{C}_{\mathsf{LSI}}}$$

37

where the first inequality follows from the triangle inequality of TV distance; the second inequality follows from Pinsker's inequality; the third inequality follows from Jensen's inequality; the fourth inequality follows from data processing inequality and the information inequality (Lemma 5) and the fifth inequality follows from Lemma 4. In order to ensure $\frac{1}{N}\sum_{i=1}^{N}\|\mu_{Kh}^i - \mu_*\|_{\mathsf{TV}} \leq \frac{1}{2}\epsilon$, it suffices to choose $T = Kh = \widetilde{\Theta}\left(\frac{\sqrt{\mathscr{L}}}{\mathscr{C}_{\mathsf{LSI}}}\right)$. In order to ensure $\frac{1}{N}\sum_{i=1}^{N}\|\bar{\mu}_K^i - \mu_{Kh}^i\|_{\mathsf{TV}} \leq \frac{1}{2}\epsilon$, it suffices to choose the stepsize

$$h = \Theta\left(\frac{\mathscr{C}_{\mathsf{LSI}}^{1/2}\epsilon}{\mathscr{L}^{5/4}T^{1/2}d^{1/2}}\right) = \widetilde{\Theta}\left(\frac{\mathscr{C}_{\mathsf{LSI}}\epsilon}{\mathscr{L}^{3/2}d^{1/2}}\right), \tag{70}$$

the mixing time

$$K = \frac{T}{h} = \widetilde{\Theta}\left(\frac{\mathscr{L}^2 d^{1/2}}{\mathscr{C}_{\mathsf{LSI}}^2\epsilon}\right), \tag{71}$$

and the number of particles

$$N = \Theta\left(\frac{\mathscr{L}^2 d}{\mathscr{C}_{\mathsf{LSI}}^2\epsilon^2}\right). \tag{72}$$

The choice of T, h, K, N above ensures $\frac{1}{N}\sum_{i=1}^{N}\|\bar{\mu}_K^i - \mu_*\|_{\mathsf{TV}} \leq \epsilon$.

F Experimental settings

In our experiment, we use a mean-field two-layer neural network to approximate the Gaussian function,

$$f(z) = \exp\left(-\frac{\|z - m\|^2}{2d}\right).$$

We uniformly draw $m \sim \mathcal{N}(0, I_d)$ and 100 points $\{z_i\}_{i=1}^{100} \sim \mathcal{N}(0, I_d)$ with $d = 10^3$ and calculate the corresponding labels $\{f(z_i)\}_{i=1}^{100}$. In this section, we give the actual updates of the methods involved in our experiment and provide the precise value of parameters in Table 2. The update of the NULA is given by

$$x_{k+1}^j = x_k^j + \varphi_0\, v_k^j - \varphi_1\, D_\mu F(\mu_{\mathbf{x}_k}, x_k^j) + \eta \xi_k^x,$$
$$v_{k+1}^j = \varphi_2\, v_k^j - \varphi_3\, D_\mu F(\mu_{\mathbf{x}_k}, x_k^j) + \eta \xi_k^v.$$

for $j = 1, ..., N$. The update of EM-N-ULA is given by

$$x_{k+1}^j = x_k^j + h_2\, v_k^j,$$
$$v_{k+1}^j = (1 - h_3)v_k^j - h_2\, D_\mu F(\mu_{\mathbf{x}_k}, x_k^j) + \sqrt{2\lambda_2 h_2}\xi_k.$$

for $j = 1, ..., N$. The update of the N-LA is given by

$$x_{k+1}^j = x_k^j - h_1\, D_\mu F(\mu_{\mathbf{x}_k}, x_k^j) + \sqrt{2\lambda_1 h_1}\xi_k.$$

for $j = 1, ..., N$.

Parameters	φ_0	φ_1	φ_2	φ_3	η	h_1	h_2	h_3	λ_1	λ_2
Value	10^{-4}	0.02	0.99	0.02	10^{-3}	10^{-2}	10^{-2}	10^{-2}	10^{-4}	10^{-4}

Table 2: Choice of hyperparameters.

G Methods for comparisons

In this section, we review the convergence result of MLA in Nitanda et al. (2022) and N-LA in Suzuki et al. (2023), which consider problem (1) in more specific settings. Nitanda et al. (2022) suppose $F(\rho) = \mathbb{E}_{(a,b)\sim\mathcal{D}}[\ell(h(\rho;a),b)] + \frac{\lambda'}{2}\mathbb{E}_{x\sim\rho}\|x\|^2$ whereas Suzuki et al. (2023) suppose $F(\rho) = U(\rho) + \lambda'\mathbb{E}_{x\sim\rho}[r(x)]$. While our convergence results are established in TV distance, we consider more general settings compared with the previous two. Since the problem setting in Nitanda et al. (2022) is only for training neural networks, we perform convergence analysis of the MLA in Suzuki et al. (2023)'s setting to make a comparison with our results. Define the free energy

$$E(\rho) = F(\rho) + \text{Ent}(\rho), \tag{73}$$

where $\mu \in \mathcal{P}_2(\mathbb{R}^d)$. Let $\bar{\rho}_k$ denotes the law of k-th iterate of the MLA and ρ_* denotes the minimizer of (73), and Nitanda et al. (2022) obtain the following results in Theorem 2:

$$E(\bar{\rho}_k) - E(\rho_*) \leq \exp(-\mathscr{C}_{\text{LSI}}hk)(E(\bar{\rho}_0) - E(\rho_*)) + \frac{\delta_h}{2\mathscr{C}_{\text{LSI}}}, \tag{74}$$

where $\delta_{hk} := \mathbb{E}\|D_\rho F(\bar{\rho}_{k+1}, x_{k+1}) - D_\rho F(\bar{\rho}_k, x_k)\|^2$ and $\mathbb{E}$ is taken under the joint law of $\bar{\rho}_{k+1}$ and $\bar{\rho}_k$. Now we bound δ_{hk} uniformly in k with a different method from the one in Nitanda et al. (2022). We do not need to specify F to be the objective of training nerual networks. Since F is $\mathscr{L}$-smooth[3] and satisfies Assumption 2.4, we obtain

$$
\begin{aligned}
\mathbb{E}\|D_\rho F(\bar{\rho}_{k+1}, x_{k+1}) - D_\rho F(\bar{\rho}_k, x_k)\|^2 &\leq 2\mathscr{L}^2\mathbb{E}(\|x_{k+1} - x_k\|^2 + W_2^2(\bar{\rho}_{k+1}, \bar{\rho}_k)) \\
&\leq 4\mathscr{L}^2\mathbb{E}\|x_{k+1} - x_k\|^2 \\
&= 4\mathscr{L}^2\mathbb{E}\| - hD_\rho F(\bar{\rho}_k, x_k) + \sqrt{2h}\xi\|^2 \\
&\leq 4\mathscr{L}^2 h^2\mathbb{E}\|D_\rho F(\bar{\rho}_k, x_k)\|^2 + 8\mathscr{L}^2 hd \\
&\leq 8\mathscr{L}^4 h^2(1 + \mathbb{E}\|x_k\|^2) + 8\mathscr{L}^2 hd
\end{aligned}
$$

We refer to Lemma 1 in Suzuki et al. (2023) to uniformly bound $\mathbb{E}\|x_k\|^2$. Before applying Lemma 1, we translate some constants in Suzuki et al. (2023) into our constants systems. Suzuki et al. (2023) assumes that $\|D_\rho U(\rho, x)\| \leq R$, $\lambda_1 I_d \preceq \nabla^2 r(x) \preceq \lambda_2 I_d$. We let $R = \mathscr{L}$ and $\lambda_2 = \mathscr{L}$ (since this specification matches our Assumption 2.4). We prove Lemma 1 proposed by Suzuki et al. (2023) in the mean-field setting without particle approximation. But we also assume the decomposition $F(\rho) = U(\rho) + \mathbb{E}_{x\sim\rho}[r(x)]$ with $\|D_\rho U(\rho, x)\| \leq \mathscr{L}$ and $\lambda_1 I_d \preceq \nabla^2 r \preceq \mathscr{L} I_d$. Given the update of the MLA, if $h \leq \frac{\lambda_1}{2\mathscr{L}^2}$, we have

$$
\begin{aligned}
\mathbb{E}\|x_{k+1}\|^2 &= \mathbb{E}\|x_k\|^2 + h^2\mathbb{E}\|D_\rho F(\rho_k, x_k)\|^2 + 2hd - 2h\mathbb{E}\langle x_k, D_\rho U(\rho_k, x_k) + \nabla r(x_k)\rangle \\
&\leq \mathbb{E}\|x_k\|^2 + \mathscr{L}^2 h^2(1 + \mathbb{E}\|x_k\|^2) + 2hd + 2h\mathscr{L}\mathbb{E}\|x_k\| - 2h\lambda_1\mathbb{E}\|x_k\|^2 \\
&\leq (1 - \lambda_1 h)\mathbb{E}\|x_k\|^2 + \mathscr{L}^2 h^2 + 2hd + \frac{2\mathscr{L}^2 h}{\lambda_1}
\end{aligned}
$$

Recursively, we obtain

$$\mathbb{E}\|x_k\|^2 \leq (1 - \lambda_1 h)^k\mathbb{E}\|x_0\|^2 + \frac{\mathscr{L}^2 h + 2d}{\lambda_1} + \frac{2\mathscr{L}^2}{\lambda_1^2} \leq \mathbb{E}\|x_0\|^2 + \frac{\mathscr{L}^2 h + 2d}{\lambda_1} + \frac{2\mathscr{L}^2}{\lambda_1^2}. \tag{75}$$

---

[3]We inherit the weaker smoothness assumption in Suzuki et al. (2023) with respect to W_2 distance.

If $x_0 \sim \mathcal{N}(0, I_d)$, $\mathbb{E}\|x_0\|^2 \lesssim d$. Thus (75) implies $\mathbb{E}\|x_k\|^2 \lesssim \mathscr{L}^2 d$. Plugging into the inequality above, we obtain

$$\mathbb{E}\|D_\rho F(\bar{\rho}_{k+1}, x_{k+1}) - D_\rho F(\bar{\rho}_k, x_k)\|^2 \lesssim \mathscr{L}^6 h^2 d + \mathscr{L}^2 h d. \tag{76}$$

Applying Lemma 3 and pinsker's inequality, we obtain

$$\|\bar{\rho}_K - \rho_*\|_{\mathsf{TV}} \lesssim \sqrt{\mathsf{KL}(\bar{\rho}_K \| \rho_*)} \leq \sqrt{E(\bar{\rho}_K) - E(\rho_*)}$$

$$\lesssim \exp(-\mathscr{C}_{\mathsf{LSI}} h K / 2)(E(\bar{\rho}_0) - E(\rho_*))^{1/2} + \frac{\mathscr{L}^3 h d^{1/2}}{\mathscr{C}_{\mathsf{LSI}}^{1/2}} + \frac{\mathscr{L} h^{1/2} d^{1/2}}{\mathscr{C}_{\mathsf{LSI}}^{1/2}}$$

In order to ensure $\|\bar{\rho}_K - \rho_*\|_{\mathsf{TV}} \leq \epsilon$, it suffices to choose

$$h = \Theta\left(\frac{\mathscr{C}_{\mathsf{LSI}}\epsilon^2}{\mathscr{L}^3 d}\right), \quad K = \widetilde{\Theta}\left(\frac{\mathscr{L}^3 d}{\mathscr{C}_{\mathsf{LSI}}^2 \epsilon^2}\right). \tag{77}$$

Now we translate the convergence results in Suzuki et al. (2023). Define the free energy of the particle system:
$$E^N(\mu^N) = N\mathbb{E}_{\mathbf{x} \sim \mu^N} F(\mu_{\mathbf{x}}) + \mathrm{Ent}(\mu^N), \tag{78}$$

where $\mu_{\mathbf{x}} = \frac{1}{N}\sum_{i=1}^N \delta_{x^i}$. Similar to the analysis above, Theorem 2 in Suzuki et al. (2023) implies the TV-convergence of the N-LA, given by

$$\frac{1}{N}\sum_{i=1}^N \|\bar{\rho}_K^i - \rho_*\|_{\mathsf{TV}} \lesssim \sqrt{\frac{1}{N}\sum_{i=1}^N \mathsf{KL}(\bar{\rho}_K^i \| \rho_*)} \leq \sqrt{\frac{1}{N}E^N(\rho_K^N) - E(\rho_*)}$$

$$\lesssim \exp\left(-\mathscr{C}_{\mathsf{LSI}} h K / 4\right) + h^{1/2} K^{1/2}(\mathscr{L}^3 h d^{1/2} + \mathscr{L} h^{1/2} d^{1/2})$$

$$+ h^{1/2} K^{1/2}\frac{\mathscr{L}^2 d^{1/2}}{N^{1/2}}$$

In order to ensure $\|\bar{\rho}_K - \rho_*\|_{\mathsf{TV}} \leq \epsilon$, it suffices to choose

$$h = \Theta\left(\frac{\mathscr{C}_{\mathsf{LSI}}\epsilon^2}{\mathscr{L}^3 d}\right), \quad K = \widetilde{\Theta}\left(\frac{\mathscr{L}^3 d}{\mathscr{C}_{\mathsf{LSI}}^2 \epsilon^2}\right), \quad N = \Theta\left(\frac{\mathscr{L}^4 d}{\mathscr{C}_{\mathsf{LSI}}\epsilon^2}\right). \tag{79}$$